Electronic-oscillator analysis of femtosecond four-wave mixing in conjugated polyenes

T. Meier, S. Tretiak, V. Chernyak, and S. Mukamel
Department of Chemistry and Rochester Theory Center for Optical Science and Engineering, University of Rochester, Rochester, New York 14627
(Received 1 July 1996)

Equations of motion which describe the nonlinear optical response of conjugated polyenes using a collective electronic-oscillator representation are derived. Specific signatures of electronic correlations which enter as anharmonicities and scattering between oscillators are predicted in ultrafast resonant four-wave mixing. Only few resonant oscillators need to be considered explicitly; effects of the remaining (off-resonant) oscillators are introduced via renormalized anharmonic coupling coefficients. The connection with inorganic semiconductors is established. [S0163-1829(97)05504-5]

I. INTRODUCTION

Nonlinear optical spectroscopy of organic materials is an intensively developing field. It constitutes both fundamental interest and potential practical applications. Compared to inorganic semiconductors, investigations of organic molecules are more difficult theoretically due to the complicated electronic structure and experimentally due to problems related to sample quality, controlled synthesis, and poor solubility of large molecules.[1,2] Resonant time domain nonlinear spectroscopy provides direct information on the creation of carriers and excitons and their subsequent dynamics.[3–7] Femtosecond time-resolved absorption spectroscopy revealed the strong coupling between electronic and vibrational states in excited state dynamics of the singlet exciton of polydiacetylene.[3] Time-resolved gain and absorption measurements have been performed to study the quantum yield of poly(paraphenylenevinylene) for films, dilute blends and solutions, the defect quenching of luminescence, the formation and decay of excitons,[4] and the energy relaxation and field-induced exciton dissociation.[5] Degenerate four-wave mixing measurements have been performed in perylenes.[6] Recently, the dephasing dynamics of vibronic states in polydiacetylene films has been investigated.[7] These experiments are usually interpreted by simply applying kinetic equations for excited state populations using phenomenological decay rates.

The calculation of electronic excitations in conjugated polyenes constitutes a complex many-body problem due to the strong correlation effects expected for one dimensional electronically delocalized systems. Exact *ab initio* quantum chemistry methods[8–10] look at effects of correlations through the positions of energy levels and the transition dipole moments. These methods are limited to small systems. The time-dependent Hartree-Fock[11] (TDHF) approach offers a convenient scheme for studying correlation effects in much larger systems. The method is not exact and neglects ground state correlations, however, it includes some important excited state correlation effects, which in many cases dominate the response. The approach further provides a classical electronic oscillator picture for the optical response.[12] This allows the development of physical insight and establishes a connection between chemical structure and optical nonlinearities, which is not available through traditional approaches based on eigenstates. This method has been successfully applied to several conjugated systems; details of the advantages of this approach as well as its limitations can be found in Refs. 12–15.

In this paper we investigate how ultrafast resonant four-wave mixing (FWM) can be used to provide some alternative, dynamical, signatures of electronic correlations. Our analysis is based on the recently developed coupled electronic oscillator representation of the optical response, obtained by following the dynamics of the reduced single electron density matrix.[12] We expand the equations of motion for the density matrix in terms of amplitudes of the various electron-hole oscillators. With these equations the optical response is mapped onto a set nonlinear equations; optical nonlinearities are attributed to anharmonicities and scattering of oscillators.[12–14] The equations of motion derived here hold for the optical response up to the third order in the incoming field. However, extending the present framework to higher order nonlinearities is straightforward.

We have applied this technique to the calculation of a specific resonant time-domain experiment, namely degenerate FWM in the two-pulse self-diffraction setup. We consider the signal generated in the $2\mathbf{k}_2-\mathbf{k}_1$ direction, where $\mathbf{k}_2$ and $\mathbf{k}_1$ are the incoming wave vectors. We assume resonant excitation of the lowest $1B_u$ oscillator and identify the oscillators which contribute to this signal. Electronic correlations, which manifest themselves as nonlinear couplings between oscillators, lead to distinct signatures in the FWM signal. Our analysis shows that for the signal considered here, only two oscillators have to be considered explicitly, which allows for a very clear and intuitive description of the various nonlinearities.[16] We shall refer to these as the primary oscillators. All other oscillators are excited off-resonance. Their dynamics follow adiabatically the excitation and therefore they can be eliminated from the equations, which results in new anharmonic couplings as well as renormalizations of the existing anharmonicities of the primary oscillators.

To analyze the time-domain signatures of correlations, we compare calculations made using the simple Hückel (SSH) model,[17] which includes no correlations in the optical response, with the Pariser-Parr-Pople (PPP) model, where Coulomb interactions are included. We find some unique sig-

natures of correlations in the ultrafast signals. First, due to correlations the shape of the FWM amplitude is changed from a free-induction decay, which has a maximum immediately after the excitation, to one which displays a delayed maximum as function of time. The results are compared with inorganic semiconductor nanostructures, where such effects have been predicted[18–20] and observed.[21,22] Second, the correlations also strongly affect the dynamics of the phase of the FWM signal. The relative phase of the FWM signal with respect to the exciting pulses changes from $\pi/2$ for the Hückel model to about 0 or π, depending on the signs of the anharmonic coupling coefficients. Third, for the PPP model we find strong signals for negative delays (pulse $\mathbf{k}_2$ comes first), which are absent in a simple two-level model. Such signals reflect the contributions of a third level which could either be a two-photon A_g oscillator or a many body effect of two B_u oscillators.[23,24] Our calculations show that anharmonicities due to many-particle interactions dominate these signals in conjugated polyenes. This state of affairs is reminiscent of molecular aggregates and was recently analyzed for photosynthetic antenna complexes.[25]

II. THE COUPLED ELECTRONIC OSCILLATOR REPRESENTATION

We consider a system of many π electrons described by the tight-binding PPP Hamiltonian, which reproduces many important properties of conjugated polyenes[26]

$$\hat{H}=\sum_{m,n,\sigma} t_{mn}c^{+}_{m,\sigma}c_{n,\sigma}+\frac{1}{2}\sum_{m,n,\sigma,\sigma'} V_{nm}c^{+}_{m,\sigma}c^{+}_{n,\sigma'}c_{n,\sigma'}c_{m,\sigma} -E(t)\sum_{n,\sigma}\mu_{nn}c^{+}_{n,\sigma}c_{n,\sigma}, \tag{1}$$

where $c^{+}_{m,\sigma}$ ($c_{m,\sigma}$) is the creation (annihilation) operator of a π electron on site m with spin σ and $\hat{\rho}^{\sigma}_{nm}=c^{+}_{m,\sigma}c_{n,\sigma}$ is the reduced single-electron density matrix.

The first term is the Hückel Hamiltonian where t_{nn} is the Coulomb integral at the nth atom [$t_{nn}=\Sigma_m V_{nm}$; t_{mn} ($m\neq n$) is the nearest-neighbor transfer integral between nth and mth atoms] $t_{n,n\pm1}=\beta_0-\beta_1 l_n$ and l_n is the deviation of the nth bond length from the mean bond length along the chain. The second term includes electron-electron Coulomb interactions. The repulsion between the nth and mth sites V_{nm} is given by the Ohno formula

$$V_{nm}=\frac{U}{\sqrt{1+(r_{nm}/a_0)^2}} \tag{2}$$

representing the variation of the repulsion between the nth and mth site with distance; here the on-site Hubbard repulsion between the nth and mth sites U is given by $U=U_0/\epsilon$, and ϵ is the static dielectric constant. The last term represents the coupling to and external electric field $E(t)$. We assume a localized basis set so that the dipole moment is diagonal $\mu_{nm}=ez_n\delta_{nm}$. The dipole operator is given by

$$\mu=\sum_{n,\sigma}\mu_{nn}c^{+}_{n,\sigma}c_{n,\sigma}. \tag{3}$$

We further assume that ground state is a singlet, and can be described by the HF single electron density matrix $\overline{\rho_{nm}}$, so that the spin variables may be eliminated.[12]

The parameters used were adjusted to reproduce the energy gap for polyacetylene (2.0 eV): $U_0=11.13$ eV, $\beta_0=-2.4$ eV, $\beta_1=-3.5$ eV Å^{-1}, $\epsilon=1.5$, $a_0=1.2935$ Å.[13] For comparison, we also performed calculations using the Hückel model where the Coulomb interaction is neglected, $U_0=0$. In this case we used $\beta_1=-5$ eV Å^{-1} in order to reproduce the PPP band edge.

The TDHF technique[11] maps the calculation of the optical response onto the dynamics of coupled electronic oscillators representing the electron-hole pair components of the reduced single electron density matrix.[12] We first find the Hartree-Fock (HF) ground state. The stationary HF density matrix $\overline{\rho}$ satisfies

$$[h(\overline{\rho}),\overline{\rho}]=0, \tag{4}$$

where

$$h(\overline{\rho})=t+V(\overline{\rho}), \tag{5}$$

$$V(\overline{\rho})_{mn}=-V_{mn}\overline{\rho_{mn}}+2\delta_{mn}\sum_l V_{ml}\overline{\rho_{ll}}. \tag{6}$$

h is the Fock operator and V is the Coulomb operator. Equation (4) can be solved by an iterative diagonalization. We have calculated the geometry optimized HF ground state[27] as described in Ref. 13.

When the polyene is driven by an external field, the density matrix becomes time dependent. We shall represent it as

$$\rho(t)=\overline{\rho}+\xi(t)+T[\xi(t)]. \tag{7}$$

Here, ξ represents the particle-hole and $T(\xi)$ is the particle-particle and the hole-hole parts of deviation of the reduced single-electron density matrix from the ground state $\overline{\rho}$. All quantities in Eq. (7) are $N\times N$ matrices, where N is the basis set size. In this scheme, which is valid in the absence of pure dephasing, the particle-particle and hole-hole components of the density matrix need not to be considered as independent variables, since they can be expressed in terms of the particle-hole part.[12] Therefore only the particle-hole components of the density matrix, ξ, need to be calculated explicitly.

T can be expanded in a Taylor series which contains only even powers of ξ. For optical signals not higher than $\chi^{(3)}$ it is sufficient to retain only the lowest (second order) term

$$T(\xi)=\tfrac{1}{2}[[\xi,\overline{\rho}],\xi]. \tag{8}$$

The equation of motion for the particle-hole part of the density matrix is given by ($\hbar=1$):

$$i\frac{\partial}{\partial t}\xi(t)=L(\xi)-E[\mu,\overline{\rho}+\xi+T(\xi)]+[V(\xi),\xi] +[V(\xi),T(\xi)]+[V(T(\xi)),\xi]+[V(T(\xi)),\overline{\rho}], \tag{9}$$

where the Liouville space operator (superoperator) L represents the linear part of the equation[13]

$$L(\xi)=[t+V(\overline{\rho}),\xi]+[V(\xi),\overline{\rho}]. \tag{10}$$

The induced-polarization [neglecting the equilibrium polarization $\mathrm{Tr}(\mu\overline{\rho})$, which does not affect in the optical response] is given by the sum of its particle-hole and particle-particle contributions

$$P[\xi(t)]=\mathrm{Tr}[\mu\xi(t)]+\mathrm{Tr}\{\mu T[\xi(t)]\}, \tag{11}$$

where μ is the dipole operator defined in Eq. (3), and $\xi(t)$ is the time-dependent driven electron-hole part of the density matrix.

A. Equations of motion for electron-hole oscillators

As shown in Ref. 12 the particle-hole part of the density matrix can be expanded on terms of modes ξ_α

$$\xi(t)=\sum_{\alpha>0}[\xi_\alpha z_\alpha(t)+\xi_\alpha^+ z_\alpha^*(t)]. \tag{12}$$

Each oscillator α is described by two operators ξ_α and ξ_α^+. These oscillator variables are related to the oscillator coordinate $Q_\alpha=(1/\sqrt{2})(\xi_\alpha+\xi_\alpha^+)$ and the momentum $P_\alpha=(i/\sqrt{2})(\xi_\alpha-\xi_\alpha^+)$.[12] As in Ref. 12 we define $\xi_{-\alpha}=\xi_\alpha^+$. z_α and its complex conjugate $z_{-\alpha}=z_\alpha^*$ will be denoted as complex oscillator amplitudes. The oscillator variables are the eigenmodes of the linear part of Eq. (9) and satisfy

$$L(\xi_\alpha)=\Omega_\alpha\xi_\alpha,\quad L(\xi_{-\alpha})=-\Omega_\alpha\xi_{-\alpha}. \tag{13}$$

They are normalized using the condition

$$\mathrm{Tr}(\overline{\rho}[\xi_{-\alpha},\xi_\alpha])=1. \tag{14}$$

Inserting the expansion Eq. (12) into Eq. (9) gives the following equations for the complex amplitude $z_\alpha(t)$ of the oscillator variable ξ_α:

$$i\frac{\partial}{\partial t}z_\alpha=\Omega_\alpha z_\alpha-E\mu_\alpha-E\sum_\beta\mu_{\alpha,\beta}z_\beta-E\sum_{\beta\gamma}\mu_{\alpha,\beta\gamma}z_\beta z_\gamma$$
$$+\sum_{\beta\gamma}V_{\alpha,\beta\gamma}z_\beta z_\gamma+\sum_{\beta\gamma\delta}V_{\alpha,\beta\gamma\delta}z_\beta z_\gamma z_\delta, \tag{15}$$

with

$$\mu_\alpha=\mathrm{Tr}([\overline{\rho},\xi_{-\alpha}][\mu,\overline{\rho}]),$$
$$\mu_{\alpha,\beta}=\mathrm{Tr}([\overline{\rho},\xi_{-\alpha}][\mu,\xi_\beta]),$$
$$\mu_{\alpha,\beta\gamma}=\mathrm{Tr}([\overline{\rho},\xi_{-\alpha}][\mu,\tfrac{1}{2}[[\xi_\beta,\overline{\rho}],\xi_\gamma]]), \tag{16}$$
$$V_{\alpha,\beta\gamma}=\mathrm{Tr}([\overline{\rho},\xi_{-\alpha}][V(\xi_\beta),\xi_\gamma])+\mathrm{Tr}([\overline{\rho},\xi_{-\alpha}]$$
$$\times[V(\tfrac{1}{2}[[\xi_\beta,\overline{\rho}],\xi_\gamma]),\overline{\rho}]),$$
$$V_{\alpha,\beta\gamma\delta}=\mathrm{Tr}([\overline{\rho},\xi_{-\alpha}][V(\tfrac{1}{2}[[\xi_\beta,\overline{\rho}],\xi_\gamma]),\xi_\delta])+\mathrm{Tr}([\overline{\rho},\xi_{-\alpha}]$$
$$\times[V(\xi_\delta),\tfrac{1}{2}[[\xi_\beta,\overline{\rho}],\xi_\gamma]]).$$

Equation (15) constitutes the equations of motion for z_α with $\alpha>0$. The amplitudes for the adjoint (negative frequency) variables are simply the complex conjugates, see Eq. (12). The summation indices β, γ, and δ on the right hand side of Eq. (15) run over all (positive and negative frequency) oscillator variables.

The first two terms in the right hand side of Eq. (15) represent a linearily driven harmonic oscillator. The other terms are anharmonicities describing coupling among electronic oscillators. We label field-induced and purely material anharmonic coefficients by μ and V, respectively. Note that the summations on the right hand side include terms where the summation indices are equal ($\beta=\gamma=\delta$) (diagonal anharmonicities). It is important to note that, as is evident from Eq. (16), all the anharmonic coefficients can be calculated using the ground state density matrix $\overline{\rho}$ as well as the eigenmodes ξ_α of the linearized TDHF equation.

The optical polarization is given by

$$P(t)=\sum_\beta\tilde{\mu}_\beta z_\beta(t)+\sum_{\beta\gamma}\tilde{\mu}_{\beta\gamma}z_\beta(t)z_\gamma(t) \tag{17}$$

with

$$\tilde{\mu}_\beta=\mathrm{Tr}(\mu\xi_\beta),$$
$$\tilde{\mu}_{\beta\gamma}=\mathrm{Tr}(\mu\tfrac{1}{2}[[\xi_\beta,\overline{\rho}],\xi_\gamma]). \tag{18}$$

As in Eq. (15) also in Eq. (17) the summation indices β and γ run over all oscillator variables. Equations (15) and (17) may be used to compute the optical response of our many-electron system. This task has therefore been mapped onto finding the oscillators and the nonlinear couplings μ and V. μ describes optical transitions between the oscillators whereas V describes scattering between oscillators, induced by the many-body Coulomb-interaction.

For a polyacetylene chain with N carbon atoms and N π electrons there are $N^2/4$ particle-hole oscillators. Equation (15) therefore represents the equations of motion for the $N^2/4$ complex amplitudes of oscillator variables associated with positive frequencies. In Ref. 12 equivalent equations of motion have been given for the coordinate Q_α and the momentum P_α of the oscillators. In the analysis of resonant optical nonlinearities it is more convenient to use the complex amplitudes, rather than coordinates and momenta. The expansion of the density matrix in the wave-vectors of the exciting fields, which corresponds to an expansion with respect to the central excitation frequencies, is simpler in this case. The equations used in Ref. 28 contain also particle-particle and hole-hole oscillators to a total number of N^2. These equations are also equivalent to the present ones, since within the TDHF the additional oscillators carry no information and can be eliminated rigorously.[12]

B. Two-oscillator representation of resonant four-wave mixing

In Appendixes A and B we show how our equations of motion can be applied to compute optical nonlinearities induced by a multiple-pulse excitation. A major advantage of the oscillator representation is that in practical applications it is usually necessary to include only very few oscillators. For off-resonant susceptibilities these are the oscillators that couple most strongly to the ground state density matrix. A tree diagram scheme for identifying the dominant oscillators for the nonlinear response, order by order, has been devel-

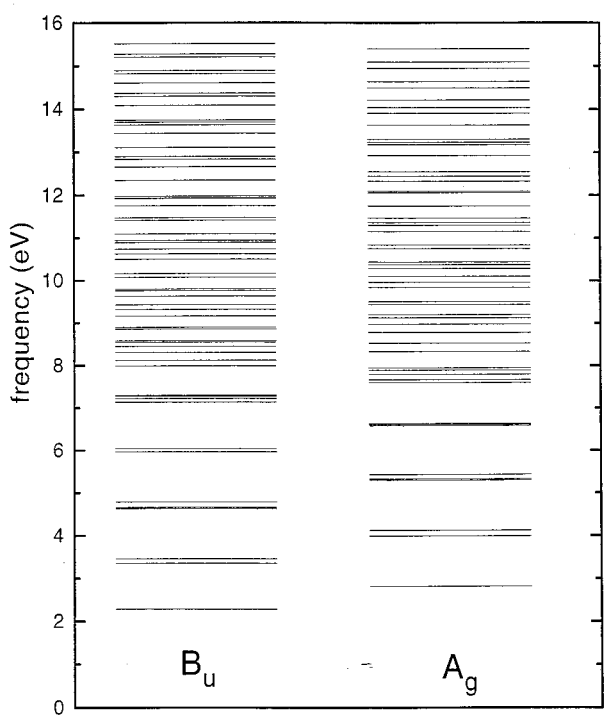

FIG. 1. Frequencies of all B_u and A_g oscillators for the Hückel model of a 30 carbon atom polyacetylene chain. There are 113 B_u and 112 A_g oscillators. The frequencies of the first eight B_u (A_g) oscillators are: 2.28, 3.35, 3.46, 3.46, 4.63, 4.66, 4.66, and 4.79 eV (2.82, 2.82, 3.99, 3.99, 4.13, 4.13, 5.30, and 5.30 eV).

oped in Ref. 28. In this paper we consider resonant response, and the most natural way to select the relevant oscillators is by including those oscillators whose frequencies are close to various combinations of the incoming field frequencies. The selectivity is expected to be more pronounced in the resonant case, which enables us to discuss the response using very few parameters (frequencies and anharmonic coefficients) connected to the relevant oscillators.

The exciting field is given by

$$E(t)=\sum_{j=1,2}\hat{E}_j e^{-[(t-\tau_j)/t_j]^2}(e^{i\mathbf{k}_j\cdot\mathbf{r}-i\omega_j t}+e^{-i\mathbf{k}_j\cdot\mathbf{r}+i\omega_j t}). \tag{19}$$

Here $\hat{E}_j$ is the real amplitude, τ_j is the time delay, and ω_j is the central frequency of pulse j. In our numerical calculations we have assumed that the central frequencies of both exciting pulses coincide with that of the $1B_u$ oscillator, which has the largest oscillator strength, i.e., $\omega_L=\omega_1=\omega_2=\Omega(1B_u)=\Omega_1$, and we used a duration of $t_1=t_2=20$ fs for the Gaussian pulse envelopes. Since the spectral width of even these very short laser pulses (about 0.1 eV) is small compared to the frequency spacing between the oscillators, only a few oscillators will be excited resonantly. Our calculations show that the first and third order response is to very good accuracy dominated by the $1B_u$ oscillator. In second order there may be one A_g oscillator which appears as resonantly excited two-photon transition. This will be discussed later using Figs. 1 and 7.

In Appendix C we have developed equations which retain only two resonantly excited primary oscillators, the $1B_u$ and one A_g oscillator, explicitly. The off-resonant contributions from all other virtual A_g oscillators in second order were adiabatically eliminated from the equations of motion, which results in renormalization of anharmonicities and scattering constants. We thus obtain the following equations of motion for the complex amplitudes of the two primary oscillators

$$\begin{aligned}i\frac{\partial}{\partial t}z_1=&\left(\Omega_1-\omega_L-i\frac{1}{T_2}\right)z_1-\mu_1 E-E^2(Y_1+X_1)z_1\\&-E^2X_{-1}z_{-1}-E\mu_{12}z_2-E(s_2+Y_3+X_3)z_1z_1\\&-E(s_1+Y_2+X_2)z_{-1}z_1\\&+2V_{12}z_2z_{-1}+(V_1+Y_4+X_4)z_{-1}z_1z_1,\end{aligned} \tag{20}$$

$$z_{-1}=z_1^*,$$

$$\begin{aligned}i\frac{\partial}{\partial t}z_2=&\left(\Omega_2-2\omega_L-i\frac{1}{T_2'}\right)z_2\\&-E\mu_{12}z_1+V_{12}z_1z_1.\end{aligned} \tag{21}$$

Here we have added phenomenological dephasing times T_2 and T_2' for the two oscillators and z_{-1} denotes the amplitude of the negative frequency variable ξ_{-1} of the $1B_u$ oscillator, see Appendix A. We assume that the relaxation times for the populations, i.e., particle-particle and hole-hole components of the density matrix, are given by $T_1=T_2/2$. We thus do not include pure dephasing processes. To investigate pure dephasing one needs to consider additional dynamic variables;[29] this goes beyond the present treatment. In principle, the inclusion of dephasing times for the off-resonant oscillators results in imaginary contributions to the renormalization terms X_i, Y_i. Since in our case the detuning for the off-resonant terms is very large compared to the dephasing rate, those imaginary parts can be neglected.

All parameters appearing in Eqs. (20) and (21) have been defined in Eqs. (C5)–(C10). In Appendix C we also present the equations in more detail, including indices denoting the propagation directions. To obtain the FWM signal we solve Eqs. (20) and (21) order by order. In first order one has to solve the equation for z_1 keeping just the $\mu_1 E$ terms on the right hand side. This represents a linearily driven harmonic oscillator with frequency Ω_1 and transition dipole μ_1. The solution of this equation yields z_1 for the propagation directions $\mathbf{k}_1$ and $\mathbf{k}_2$. z_{-1} is then the complex conjugate of z_1 with the inverse directions $-\mathbf{k}_1$ and $-\mathbf{k}_2$ (see the Appendixes). Then we solve the equation for z_2 in second order, keeping inhomogenities representing two-photon resonances, which correspond to the direction $2\mathbf{k}_2$. In the equation for z_2 the first term represents an oscillator with frequency Ω_2. The other terms are nonlinear sources. μ_{12} is a transition dipole coupling the two oscillators and V_{12} a many-body induced nonlinear coupling. Finally, the first and second order terms are inserted again into the equation for z_1 to calculate the third order $\mathbf{k}_S=2\mathbf{k}_2-\mathbf{k}_1$ component. The induced polarization in this direction is given by

$$P_S(t)=e^{-i\omega_L t}\left(\mu_1 z_1+\sum_\beta \mu_{-1\beta}z_{-1}z_\beta+\sum_\beta \mu_{1\beta}z_1z_\beta\right). \tag{22}$$

As shown in Appendix C the amplitudes for the virtual A_g oscillators be evaluated analytically. Inserting these expressions, Eqs. (C1)–(C4), into Eq. (22) simplifies the expression for the polarization,

$$\begin{aligned} P_S(t) &= e^{-i\omega_L t}[\mu_1 z_1 + \mu_{12} z_{-1} z_2 + (A_1 + B_1) z_{-1} (z_1)^2 \\ &\quad + (A_2 + B_2) E z_{-1} z_1 + A_3 E (z_1)^2] \\ &= e^{-i\omega_L t} |P_S(t)| e^{-i\varphi'(t)}. \end{aligned} \tag{23}$$

The anharmonic constants A_1, A_2, A_3, B_1, and B_2 arise from the elimination of the virtual oscillators, see Eq. (C11). $|P_S(t)|$ is the time-resolved amplitude and $\varphi'(t)$ is the slowly varying part of the phase. The total phase of the signal is given by $\varphi_S(t) = -[\omega_L t + \varphi'(t)] = -\varphi_L(t) - \varphi'(t)$, where $\varphi_L(t)$ is exactly the phase of the exciting laser pulses, see Eq. (19). We later examine the relative phase of the signal with respect to the exciting pulses[30]

$$\Delta\varphi(t) = \varphi_L(t) - \varphi_S(t) = \varphi'(t). \tag{24}$$

This phase can be measured using heterodyne detection. The time-integrated FWM signal is given by

$$S_{INT}(\tau) = \int |P_S(t)|^2 dt, \tag{25}$$

where τ is the time delay between the two pulses.

The interpretation of the various terms in Eq. (20), which generate the FWM signal, are as follows. First we discuss the terms which only involve the $1B_u$ oscillator. s_1 is the only nonlinearity which is also present in a simple two level system.[31] It represents the creation of a FWM signal by scattering of the field off a transient grating $(\mathbf{k}_2 - \mathbf{k}_1)$. It has its origin in the fact that electrons are fermions and is usually referred to as Pauli blocking or phase-space filling nonlinearity.[18,19,21] s_2 describes a similar process, where now the field is scattered off a term rotating with twice the transition frequency of the $1B_u$ oscillator $(-2\omega_2)$, instead of a transient grating term $(\omega_1 - \omega_2)$, which has no optical rotation frequency, since $\omega_1 = \omega_2$. V_1 formally appears as a local-field-like nonlinearity.[18,29] It describes self-scattering of the excitation of the $1B_u$ oscillator induced by the many-particle Coulomb-interaction. Next we discuss the terms resulting from the A_g oscillator, which is excited resonantly in second order. μ_{12} is the transition dipole which couples the A_g and $1B_u$ oscillators. It describes the creation of a third order polarization associated with the $1B_u$ oscillator, created from the excitation of the A_g oscillator times a field. μ_{12} also appears in the definition of the polarization. This term comes from the particle-particle part of the density matrix. V_{12} describes the many-particle induced coupling between the A_g and the $1B_u$ oscillator, which gives rise to nonlinear signals. All other terms (X_i and Y_i) come from the elimination of off-resonant second order contributions. X_1, Y_1, X_{-1} describe the creation of a FWM signal by scattering of a linear term by two fields. In the definition of these coefficients it follows that they are determined only by dipole moments between oscillators. All other terms resulting from the elimination process involve many-particle interactions between oscillators, which means that they are zero for the Hückel model. By inspection of the equations of motion one finds that all these terms lead to renormalizations of already existing nonlinear coupling coefficients s_1, s_2, V_1. Finally, the particle-particle part of the density matrix leads to the quadratic terms in the polarization, Eq. (22).

Depending on the time delay, the FWM technique considered here yields information about different anharmonic couplings. For positive delay (pulse $\mathbf{k}_1$ comes first) this technique is known as photon echo, since in an inhomogeneously broadened system the amplitude of the signal will have an echo-like envelope.[31,32] As can be analyzed using Eq. (C7), for a positive delay larger than the pulse duration, when the overlap between the two pulses can be neglected, only few of the inhomogentities in Eq. (20) contribute to the signal. Like in a two-level system, the phase-space filling s_1 and its renormalizations Y_2 and X_2 only contribute for positive delay.[31,32] Also, the small renormalization term X_{-1} only contributes for positive delay. All of these inhomogenities explicitly contain pulse $\mathbf{k}_2$ multiplying a term which is present after both pulses have excited the system, see Eq. (C7). This only leads to nonvanishing results, if pulse $\mathbf{k}_2$ comes after pulse $\mathbf{k}_1$. For positive delays also the many-particle induced terms represented by the nonlinear scattering potentials V_{12} and V_1, as well as its renormalizations Y_4 and X_4 contribute.[18,19] The sources of these terms do not contain an electric field, but are given by products of complex amplitudes. These amplitudes do not vanish as fast as the exciting pulses, but decay slowly as determined by the dephasing times. Therefore these many-particle terms will contribute to the signal for any time delay.[18–20]

For large negative delay the two-photon resonances induce FWM signals even if many-particle interactions are neglected.[23,24] (Note that for a linearily driven harmonic three-level system, i.e., equal energy spacing and dipole moments scaling like $\sqrt{2}$, all nonlinear terms cancel identically, and the optical response is purely linear.) This is represented by μ_{12} and s_2, as well as its renormalizations Y_3 and X_3. These inhomogeneties contain pulse $\mathbf{k}_1$ multiplying a term which is present after pulse $\mathbf{k}_2$ has excited the system, see Eq. (C7). Such terms are nonvanishing only if pulse $\mathbf{k}_1$ comes after $\mathbf{k}_2$. For a small (positive or negative) delay, when the two pulses temporarily overlap, all of the inhomogeneties in Eq. (20) contribute. In addition to the ones discussed before, also the small source terms Y_1 and X_1, may contribute to the signal. Since they contain explicitly both pulse $\mathbf{k}_1$ and $\mathbf{k}_2$ they vanish unless both pulses overlap.

III. NUMERICAL RESULTS

In this section we compare the calculated FWM signals for the Hückel and the PPP models for a 30 carbon atom polyacetylene chain. The signal will be analyzed in terms of the anharmonicities and scattering of the oscillators as described in the previous section. We tabulate all relevant coupling constants and show how many virtual oscillators are needed for calculating the renormalized anharmonicities.

TABLE I. Mode frequencies and anharmonic coupling constants for the Hückel and the PPP models.

	Hückel	PPP
$\Omega(1B_u)$	2.28 eV	2.28 eV
$\Omega(5B_u)$	3.99 eV	4.52 eV
μ_1	$3.86e$ Å	$4.80e$ Å
s_1	$-3.86e$ Å	$-2.81e$ Å
s_2	$0.0e$ Å	$0.017e$ Å
V_1	0.0 eV	0.063 eV
μ_{12}	0.0 eV	$0.66e$ Å
V_{12}	0.0 eV	-0.012 eV
X_1	$21.99e$ Å^{2}V^{-1}	$5.36e$ Å^{2}V^{-1}
X_{-1}	$0.0e$ Å^{2}V^{-1}	$0.078e$ Å^{2}V^{-1}
X_2	$0.0e$ Å	$0.26e$ Å
X_3	$0.0e$ Å	$0.13e$ Å
X_4	0.0 eV	-0.083 eV
Y_1	$-36.16e$ Å^{2}V^{-1}	$-23.0e$ Å^{2}V^{-1}
Y_2	$0.0e$ Å	$-1.33e$ Å
Y_3	$0.0e$ Å	$-0.67e$ Å
Y_4	0.0 eV	0.035 eV

A. Hückel model

We first discuss the properties of the geometry optimized ground state for the Hückel model.[13,27] The ground state is characterized by a uniform charge density $\rho_{nn}=0.5$ at each carbon atom. The second quantity, which is closely related to the stabilization mechanism of the ground state, is the bond order defined by

$$p_n=\overline{\rho}_{n,n+1}+\overline{\rho}_{n+1,n}. \tag{26}$$

We further introduce the bond order alternation parameter p_n'

$$p_n'=\langle p_n\rangle-(-1)^n p_n, \tag{27}$$

where $\langle p_n\rangle$ is the average bond order, which is 0.64 in our calculation. The geometry optimized ground state is a bond order wave, where p_n alternates between every two bonds.[13,14] Except for boundary effects near the chain ends it has an almost uniform bond order alternation parameter of $p_n'=0.21$. The average bond length is 1.06 ± 0.11 Å. Thus the transfer integral can be approximated by $t_{n,n\pm1}=\beta[1-(-1)^n\delta]$, with $\beta=-3.9$ eV and $\delta=0.13$.

For the Hückel model most of the coupling constants appearing in the equations of motion, Eqs. (20) and (21), are zero, since the Coulomb matrix vanishes, see Table I. The surviving terms μ_1,s_1,s_2,μ_{1n} do not include the Coulomb interaction. As can be seen in Appendix C, most of the terms arising from the elimination of the off-resonant A_g oscillators involve the Coulomb interaction. Therefore only X_1,X_{-1},Y_1 are finite. Additionally, for the Hückel model we find no A_g oscillator which can be resonantly excited as a two-photon resonance. This can be seen from Fig. 1, which displays the frequencies of all oscillators. The frequency of the lowest $1B_u$ oscillator is 2.28 eV. The A_g oscillators which are closest in frequency to twice the frequency of the $1B_u$ are the $6A_g$ and $7A_g$ oscillators at 4.13 eV. The frequency difference $2\Omega(1B_u)-\Omega(6A_g)=0.43$ eV is already larger than the spectral width of the exciting 20 fs laser pulses, which is about 0.1 eV. Therefore all contributions from A_g oscillators can be assumed to be off-resonant and the only primary oscillator is the $1B_u$. In the numerical calculations of the FWM signal we have included the phenomenological relaxation times $T_2=80$ fs for the B_u and $T_2'=40$ fs for the A_g oscillators.

In Figs. 2(a) and 2(b) we show the density matrices of the ground state and of the $1B_u$ oscillator using the π orbital (real-space) basis. The diagonals of these plots represent the charge density ρ_{nn}, the off diagonal elements show the electronic coherences in the system. The ground state is more localized along the diagonal than the oscillator, which shows that the optical excitation creates electronic coherence in the system.

In Table I we give the relevant coupling constants for the Hückel model. It turns out that $\mu_1=-s_1$; this resembles a simple two-level model, where the inhomogenity of the optical Bloch equation for the polarization reads $\mu E(1-n)$ (here n is the population).[31] We also find that s_2 is zero, indicating that no two-photon resonance involving solely the $1B_u$ oscillator contributes to the signal, which again mimics a simple two-level system. Therefore the only nonlinearity, involving just the $1B_u$ oscillator, is given by s_1, which represents a scattering of the field off a transient grating.

Looking at the coupling coefficients arising from the elimination of the A_g oscillators, it turns out that X_{-1} vanishes, and X_1 and Y_1 are finite. Both of these coefficients represent the scattering of two fields of the linear excitation. These terms result in small contributions to the FWM signal and, as can be seen from Eq. (C7), they only contribute when the two pulses overlap in time.

To find out how many virtual oscillators contribute to these two terms, we show in Fig. 3 the convergence of X_1 and Y_1 with the number of virtual A_g oscillator variables taken into account. The summations over the A_g oscillators, see Eq. (C10), have been made in such a way that we start with the largest term and then one by one include the smaller coupling terms. We see that by taking just 2 (out of 224) A_g oscillators variables into account to obtain a 0.5% accuracy for X_1 and 2.5% for Y_1. The two oscillators most strongly coupled to the $1B_u$ oscillator are the $2A_g$ and $3A_g$ oscillators; both have a frequency of 2.82 eV.

In Fig. 4 we display the amplitude and the relative phase of the time-resolved FWM signal for time delay $\tau=0$ fs for three different models. Model IH is a full calculation which includes all oscillators explicitly, according to Appendix B. In models IIH and IIIH only the $1B_u$ oscillator has been considered explicitly. The off-resonant A_g oscillators enter via renormalizations of the anharmonic couplings in model IIH (see Appendix C), while in model IIIH they are neglected. We find that all three calculations are very similar. Only during the excitation process, when the signal is still small, there are slight differences in the phase of the signals. This analysis shows that the resonant FWM signal for the Hückel model is well described by the $1B_u$ oscillator alone, which can also be described using a simple two-level model. The shape of the amplitude of the FWM signal represents a

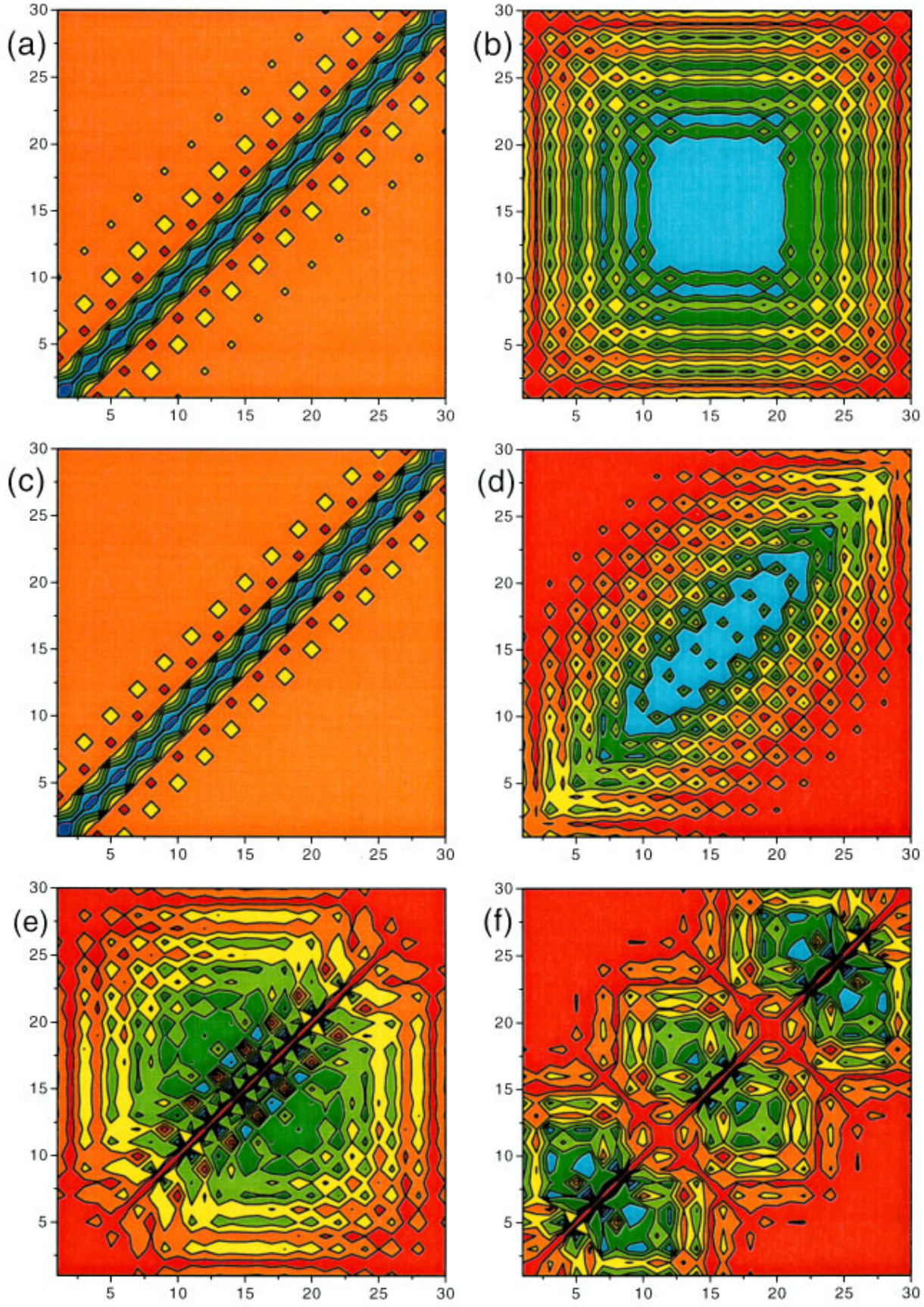

FIG. 2. (color) (a) Ground state density matrix and (b) absolute value of density matrix representing the $1B_u$ oscillator for the Hückel model. (c) Ground state density matrix and absolute value of density matrix representing the $1B_u$ (d), $3A_g$ (e), and $5A_g$ (f) oscillators for the PPP model (large is denoted by blue, green, and yellow. Small is denoted by red).

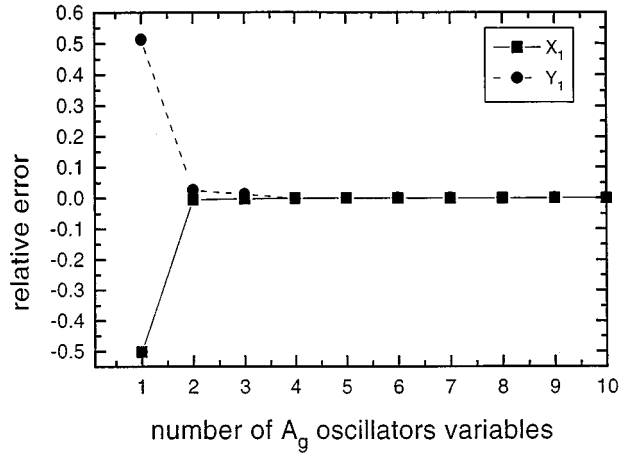

FIG. 3. Convergence of anharmonicities for the Hückel model as function of number of virtual A_g oscillator variables. Shown is the relative percent difference of the quantity to its converged value.

free-induction decay, which means that the signal reaches its maximum immediately after the excitation by the pulses, and subsequently decays.[31] We also compute the relative phase $\Delta\varphi$ of the FWM signal, which is given in Fig. 4(b), after the excitation process ($t>20$ fs) is equal to $\pi/2$. This means that, as in a resonantly excited classical oscillator, the optically excited polarization follows the laser pulse with a phase shift of $\pi/2$, which is in agreement with the analytical solution of optical Bloch equations performed for ultrashort pulses.[18,31] It has been shown that in this limit the FWM signal caused by phase-space filling has a negative imaginary prefactor, which gives a relative phase of $\pi/2$.

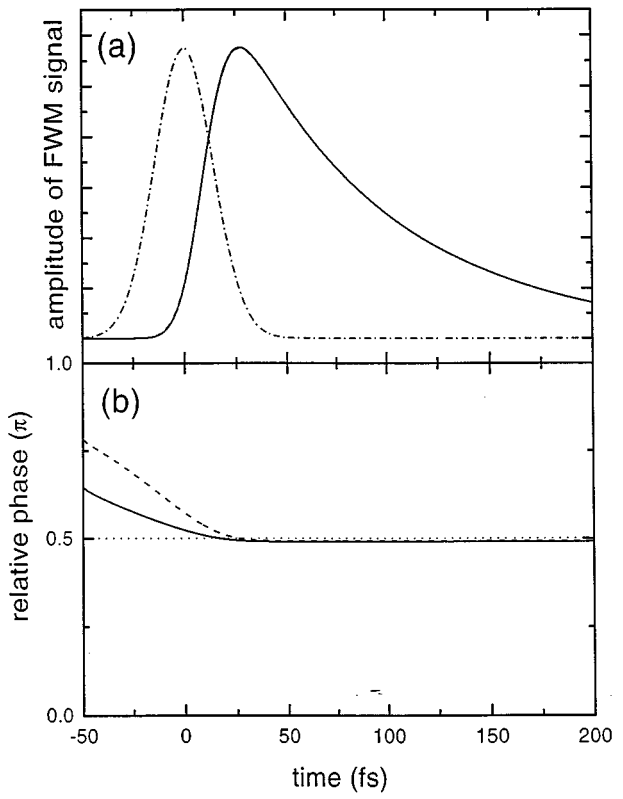

FIG. 4. (a) Time-resolved amplitude and (b) phase of the FWM signal for time-delay $\tau=0$ fs for the Hückel model. Solid line: model IH, dashed: model IIH, dotted: model IIIH, and dashed-dotted: laser pulse envelope.

The second order density matrix has a $\mathbf{k}_2-\mathbf{k}_1$ (transient-grating) and a $2\mathbf{k}_2$ (two-photon) component. The latter is negligible in the present calculation. Figure 5(a) shows the second order density matrix representing a transient grating in real space,

$$\rho^{(-1|1)}(t)=e^{i(\omega_1-\omega_2)t}\Bigg(\frac{1}{2}([[\xi_1,\overline{\rho}],\xi_{-1}] + [[\xi_{-1},\overline{\rho}],\xi_1])z_{-1}^{(-1|0)}(t)z_1^{(0|1)}(t) + \sum_\beta \xi_\beta z_\beta^{(-1|1)}(t)\Bigg). \tag{28}$$

Here, the upper indices refer to the propagation directions, see Appendix A. Due to the symmetry of this expression the density matrix ρ_{ij} representing this term is zero if $i+j$ is even (this is indicated by the red squares in Fig. 5(a), where we have used a different plot style but the same color code as in Fig. 2). The A_g oscillator amplitudes ($z_\beta^{(-1|1)}$) are small, and the odd index combinations show therefore a profile similar to the $1B_u$ oscillator shown in Fig. 2(b).

Since we have shown that the Hückel model behaves like a simple two-level system, we expect no time-integrated FWM signal for negative delays. This is verified by Fig. 6, where we compare model IH and IIIH. While the signal for positive delays decays with $T_2/2$, as expected for a homogeneously broadened two-level system, the signal decays much faster for negative delays. The small signals for negative delays solely originate from the finite pulse width. The dashed line in Fig. 6 represents the time-integrated signal for model IIIH, it lies almost exactly on the solid line representing model IH.

We should, however, point out that the absence of the second primary oscillator, appearing as a two-photon resonance is not an intrinsic property of the Hückel model. For other sizes or bond alternation parameters there may be A_g oscillators with frequencies in the vicinity of twice the frequency of the $1B_u$ oscillator, which may then also contribute to the nonlinear response. For the same parameters used here, we find that for a chain containing 22 carbon atoms the $6A_g$ and $7A_g$ oscillators can be resonantly excited as two-photon resonances [$\Omega(1B_u)=2.56$ eV, $\Omega(6A_g)=\Omega(7A_g)=5.11$ eV]. Our calculations show, that compared to the $1B_u$ oscillators, even for this case, the A_g oscillators contribute only weakly for the signal. For zero delay they are responsible for only 0.8% of the signal (for the 30 carbon atom chain this value is 0.2%). However, for large negative delays, when the contributions from the $1B_u$ oscillator vanish, the two-photon resonances induce a finite FWM signal. For the chain of 22 carbon atoms these signals for negative delays are very weak. The time-integrated FWM signal for

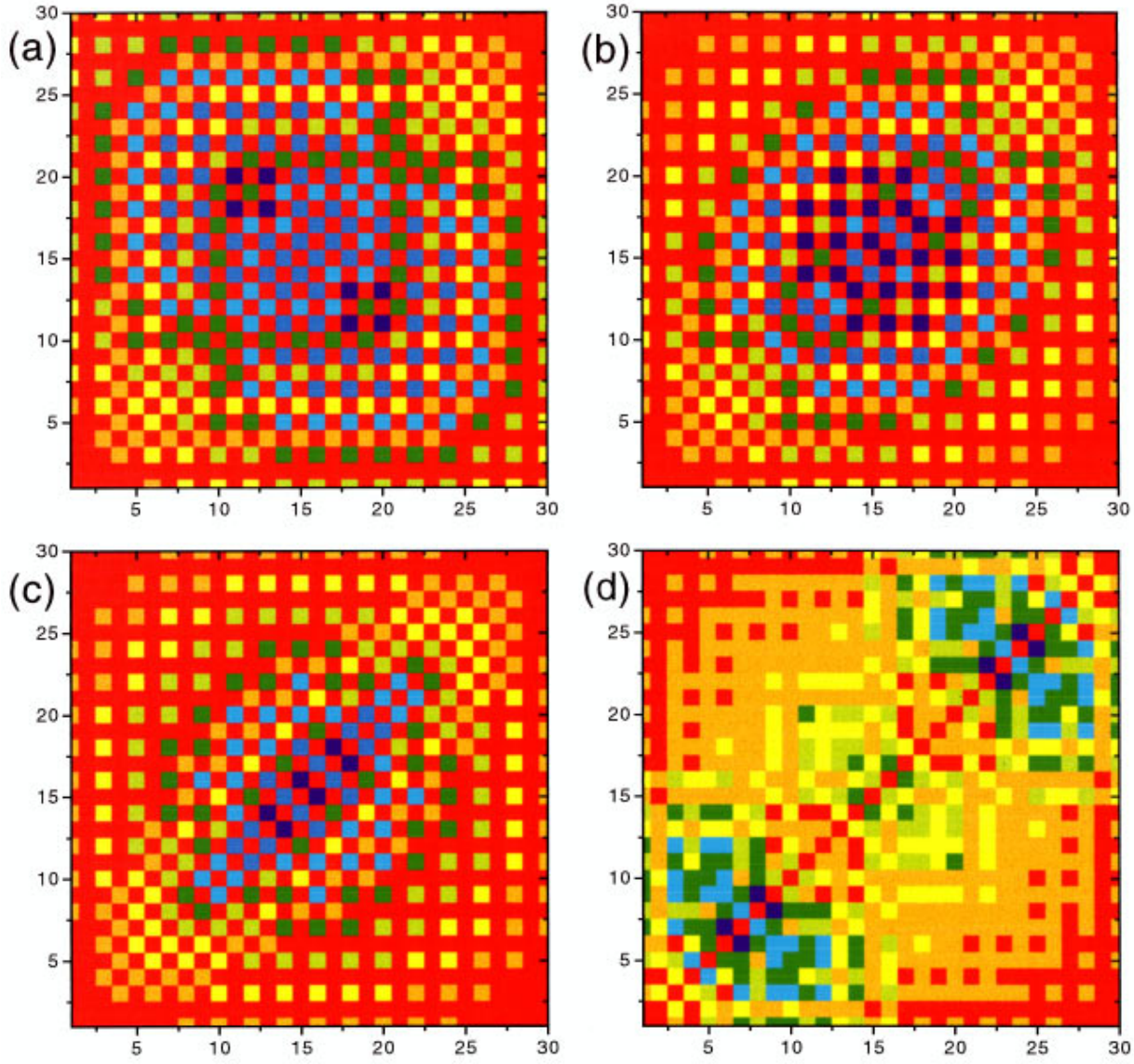

FIG. 5. (color) Absolute value of second-order density matrix $\rho^{(2)}(t)$ at $t=20$ fs representing transient-grating $(\mathbf{k}_2-\mathbf{k}_1)$ for (a) model IH, Eq. (27), (b) model IP, Eq. (28), (c) model IIP, Eq. (27), and (d) two-photon resonances $(2\mathbf{k}_2)$ for model IIIP, Eq. (29).

$\tau=-100$ fs is five orders of magnitude smaller than the one for zero delay. We therefore believe that our conclusions drawn for the resonant response of Hückel model, regarding the weak coupling of the $1B_u$ to the A_g oscillators, are of general nature.

B. PPP model

We shall now explore the role of electronic correlations by repeating the previous calculations for the PPP model. Similar to the Hückel model, the geometry optimized HF ground state is characterized by a bond order wave with a uniform charge density.[13,27] This structure is stabilized by the electron-phonon and the Coulomb exchange interactions. The calculated ground state has an average bond order $\langle p_n\rangle=0.63$ and alternation parameter $p'_n=0.24$. The average bond order alternation is a little larger than in the Hückel

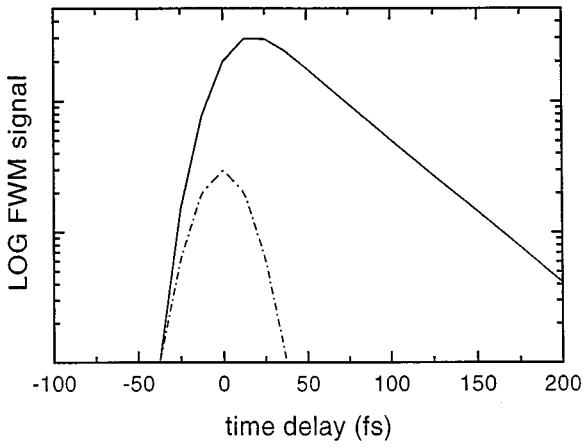

FIG. 6. Time-integrated FWM for the Hückel model. Solid line: model IH, dashed: model IIIH, and dashed-dotted: laser pulse envelope.

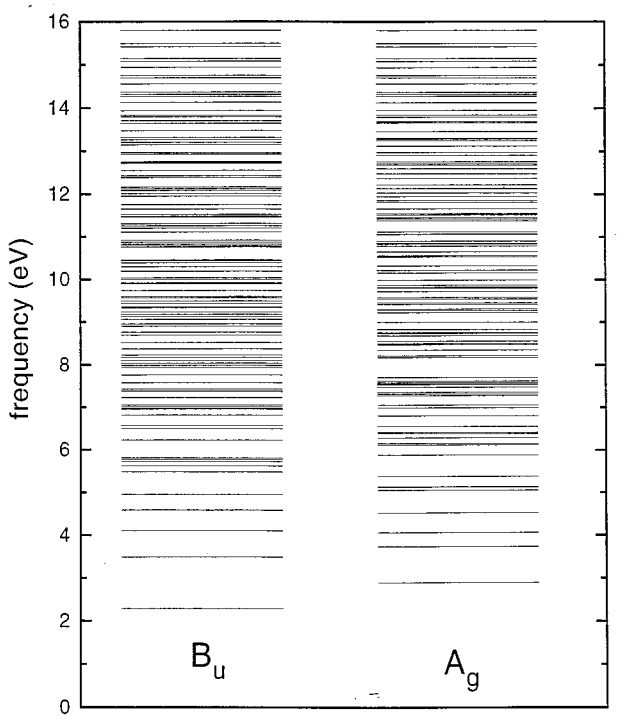

FIG. 7. B_u and A_g oscillator frequencies for the PPP model for a 30 carbon atom polyacetylene chain. There are 113 B_u and 112 A_g oscillators. The frequencies of the first eight B_u (A_g) oscillators are: 2.28, 3.49, 4.10, 4.57, 4.59, 4.95, 5.48, and 5.62 eV (2.89, 3.73, 4.06, 4.52, 5.05, 5.12, 5.13, and 5.37 eV).

model. The average bond length is 1.31 ± 0.05 Å, where the alternation is due to the larger force constant smaller than in the Hückel model.[27] The average transfer integral can be approximated by $t_{n,n\pm1}=\beta[1-(-1)^n\delta]$, with $\beta=-2.7$ eV and $\delta=0.07$.

All of the coupling constants in Eqs. (20) and (21) can contribute once the Coulomb interaction is incorporated, see Table I. The frequency of the lowest $1B_u$ oscillator is again 2.28 eV. The A_g oscillator which is closest in frequency to twice the frequency of the $1B_u$ is the $5A_g$ at 4.52 eV, see Fig. 7. The frequency difference $2\Omega(1B_u)-\Omega(5A_g)=0.049$ eV is smaller than the spectral width of the exciting 20 fs laser pulses. All other contributions from A_g oscillators can be assumed to be off resonant. So the two primary oscillators, which are considered explicitly, are $1B_u$ and $5A_g$.

In Figs. 2(c) and 2(d) we show the density matrices of the HF ground state and of the $1B_u$ oscillator. Compared to the $1B_u$ oscillator, see Fig. 2, calculated for the Hückel model, which is strongly delocalized in the off-diagonal direction, the many-particle Coulomb-interaction leads to localization of the oscillator towards the diagonal. Still the ground state is again more localized along the diagonal than the oscillator, which shows that the optical excitation creates electronic coherence in the system. Also shown in Fig. 2 are the most strongly contributing A_g oscillators, (e) the $3A_g$, which gives the strongest off resonant contribution, and (f) the $5A_g$, which appears as a two-photon resonance.

In Table I we give the relevant coupling constants for the PPP model. To simplify the analysis of these numerous terms, we split the discussion into three parts. In model IP, like in model IIIH for the Hückel model, we neglect all contributions except for the ones involving only the $1B_u$ oscillator. In addition to these contributions we include in model IIP the renormalization originating from the elimination of the A_g oscillators appearing as transient-gratings (X_i). Finally, in model IIIP we also add the explicitly considered $5A_g$ oscillator, as well as all renormalizations induced by A_g oscillators appearing as two-photon resonances (Y_i).

In model IP only the following terms contribute: μ_1, s_1, s_2, V_1. s_1 describes the phase space filling, unlike the Hückel model, due to correlations its magnitude is not equal to the magnitude of the dipole μ_1 but is somewhat smaller. s_2 describes a similar process, where now the field is scattered off a term rotating with twice the transition frequency of the $1B_u$ oscillator, instead of a transient grating term like in s_1, which basically has no rotation. In the absence of correlation (the Hückel model) s_2 was zero, here s_2 is finite, but still very small, only 0.6% of s_1, and can therefore be neglected. V_1 represents a many-particle induced scattering potential, which formally appears like a local field correction.[18–20] Actually it includes all many-particle contributions involving only the $1B_u$ oscillator. Neglecting the small s_2 contribution, the equation is equivalent to a nonlinear wave-equation, which has been extensively used for the description of nonlinear optical properties of inorganic semiconductors.[18,19,21,30] In this sense the nonlinear wave-equation appears as a special case of the present oscillator equations, obtained when some terms are neglected. This nonlinear wave equations can be derived by expanding the semiconductor Bloch equation[33,34] in an excitonic basis, keeping only the $1s$ exciton. In the language of the semiconductor Bloch equations the nonlinear scattering potential includes energy and field renormalization terms, which are induced by the many-particle Coulomb interaction.[20,30]

The FWM signal for model IP is given by the solid lines in Fig. 8, where both the amplitude of the FWM signal and its relative phase are plotted. Compared to the Hückel model calculations, the amplitude changes its shape. It is no longer a free-induction decay, but has a maximum at later times, which are determined by the dephasing times. This is the same signature that has been observed in time-resolved FWM experiments on inorganic semiconductor nanostructures.[21,22,35] In semiconductors these signal shapes have been interpreted by a nonlinear Ginzburg-Landau-like wave equation for the $1s$ exciton amplitude.[18,19,21,30] If we only consider the $1B_u$ oscillator and further neglect the small s_2 term, we obtain an identical wave equation as a special case of the oscillator equations. Besides the phase-space filling (s_1) induced by the many particle Coulomb interaction it has an additional nonlinearity (V_1), which formally appears like a local field correction. This nonlinear scattering potential describes scattering of the induced polarizations, resulting in a FWM signal. According to analytical solutions of optical Bloch equations including a local field, this contribution has a real positive prefactor.[18,30] Since V_1 itself is positive and since the many-particle induced FWM signal is like in inorganic semiconductors larger than the phase-space filling, the relative phase of the FWM signal, solid line in Fig. 8, is about 0, i.e., the induced polarization is in phase with the exciting pulse.

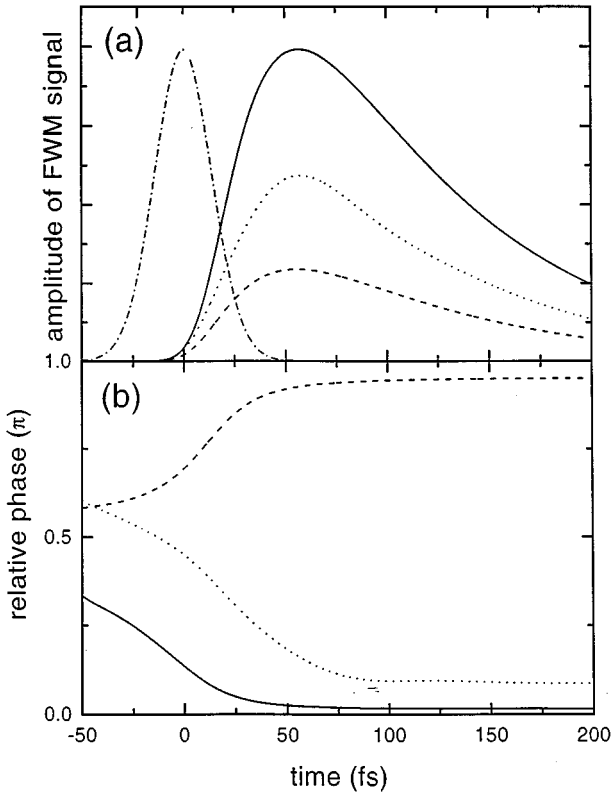

FIG. 8. (a) Time-resolved amplitude and (b) phase of the FWM signal for time-delay $\tau=0$ fs for the PPP model. Solid line: model IP, dashed: model IIP, dotted: model IIIP, and dashed-dotted: laser pulse envelope.

Figure 5(b) shows the second-order density matrix in real space, representing a transient-grating $(\mathbf{k}_2-\mathbf{k}_1)$ formed by the $1B_u$ oscillator

$$\rho^{(-1|1)}(t)=e^{i(\omega_1-\omega_2)t}\tfrac{1}{2}([[\xi_1,\overline{\rho}],\xi_{-1}]$$

$$+[[\xi_{-1},\overline{\rho}],\xi_1])z_{-1}^{(-1|0)}(t)z_1^{(0|1)}(t). \quad (29)$$

Due to the symmetry of this expression, as in the Hückel model, the density matrix ρ_{ij} representing this term is zero if $i+j$ is even (this is indicated by the red squares). The odd index combinations show a profile similar to the $1B_u$ oscillator shown in Fig. 2(d). Accordingly, like the $1B_u$ oscillator, the corresponding transient-grating is also more localized in the PPP than in the Hückel model.

In model IIP the off-resonant transient grating contributions X_1-X_4 are included. The convergence of these parameters with the number of oscillator variables is shown in Fig. 9. The value for X_1, which is a small contribution, since it describes scattering of a linear term off two-fields, is to 2.7% accuracy given by the coupling to the $3A_g$ oscillator. For X_{-1}, we have to keep five A_g oscillator variables to get 5% accuracy. X_2, which acts as a renormalization of s_1, is to within 5% given by the coupling to the $3A_g$ oscillator alone. For X_3, which acts as a renormalization of s_2, we have to

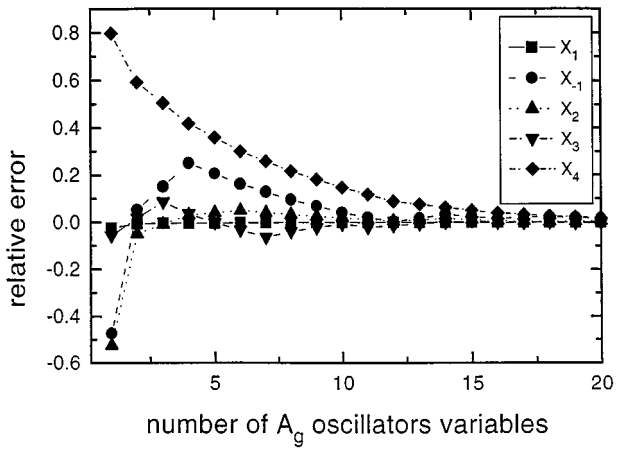

FIG. 9. Convergence of the X anharmonicities for the PPP model as function of number of virtual A_g oscillator variables. Shown is the relative percent difference of the quantity to its converged value.

keep contributions from three A_g oscillators variables to get it to 3% accuracy. To get X_4, the renormalization of the nonlinear scattering potential V_1 also within 5%, we have to keep 16 oscillator variables. The expression for X_4 is entirely determined by the Coulomb interaction between different oscillators. Its slow convergence as function of the number of oscillators variables compared to the other quantities indicates, that the Coulomb interaction couples the oscillators much less selectively than the dipole coupling, which is present in the expressions for the other terms.

The FWM signal for model IIP is given in Fig. 8 (dashed lines) where the absolute value as well as the relative phase of the FWM signal are plotted. The most notable changes between the signal involving only the $1B_u$ oscillator and the present one are the decrease in amplitude and the change in phase. These features can be simply explained by considering the values of V_1 and its renormalization X_4. While V_1 is positive $+0.063$ eV, X_4 is calculated to be negative and larger in absolute value -0.082 eV. Therefore the effective nonlinear scattering potential $V_1+X_4=-0.019$ eV is negative and about a factor 3 smaller than V_1. This reduces the amplitude of the interaction-induced contribution to the signal and changes its phase, which in turn explains the observed differences. This change of phase has strong influence on the spectrally resolved FWM signal. While the Fourier transform (FT) of the signal originating from the $1B_u$ oscillator is, like in inorganic semiconductors,[30,36] slightly asymmetric with respect to detuning with a tail towards lower frequencies, the FT of the signal for model IIP, is asymmetric with tails towards higher frequencies. These spectral features can also be analyzed using a Wigner spectrogram[37,38] as discussed in Ref. 16.

Figure 5(c) shows the transient-grating $(\mathbf{k}_2-\mathbf{k}_1)$ part of the second order density matrix in real space. It is formed by the $1B_u$ oscillator and some A_g oscillators and given by Eq. (28). The density matrix contains contributions from the $1B_u$ and about eight A_g oscillators, which contribute most strongly to X_4. ρ_{ij} is again zero if $i+j$ is even (this is indi-

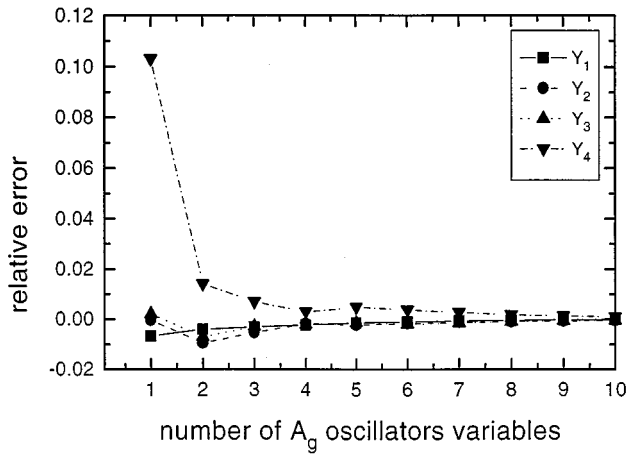

FIG. 10. Same as Fig. 11 but for the Y anharmonicities.

cated by the red squares). Due to the contributing A_g oscillators, the resulting density matrix extends further to the off-diagonal than the one originating from the $1B_u$ oscillator alone.

So far, our analysis demonstrated that the off-resonant terms involving transient gratings contribute significantly. In addition to the previous terms we include in model IIIP all renormalizations arising from terms representing two-photon resonances Y_1-Y_4. Their convergence with the number of virtual oscillators variables is shown in Fig. 10. The value for Y_1 (which is a small contribution, since it describes scattering of a linear term off two fields) is to 0.7% given by the coupling to the $3A_g$ oscillator. The value for Y_2 (Y_3), which act as renormalizations of s_1 (s_2), is to 0.1% (0.2%) given by the coupling to the $3A_g$ oscillator. The reason that we essentially only need the $3A_g$ oscillator to determine Y_1-Y_3 is that in addition to its strong dipole coupling to the $1B_u$ oscillator, it is not too much off resonant compared to most other oscillators. To get Y_4, the renormalization of the nonlinear scattering potential V_1 also within 5%, we have to keep two oscillators the $3A_g$ and the $8A_g$. As a two-photon resonance we also keep the $5A_g$ explicitly. It is dipole and Coulomb coupled to the $1B_u$ oscillator by μ_{12} and V_{12}.

The FWM signal for model IIIP is given in Fig. 8 (dotted line). Compared to model IIP, the amplitude increases again and the phase is close to 0. In order to explain these changes we have to consider two effects. First, like before, the renormalization of V_1. The effective nonlinear scattering potential is now given by $V_1+X_4+Y_4$ which is 0.016 eV, a positive but quite small value. Second, the increase in amplitude is caused by the contribution from the two-photon resonance represented by V_{12}, which describes the Coulomb coupling between the $1B_u$ and the $5A_g$ oscillator.

This change of phase will again influence the spectrally resolved FWM signal, which is now again asymmetric with respect to the detuning with tails towards negative detuning. This is the same signature which appears when we keep only the $1B_u$ oscillator, and is also the typical signature in the FT FWM signal of inorganic semiconductors.[30,36]

Figure 5(d) shows the two-photon resonance ($2\mathbf{k}_2$) part of the density matrix in real space, which is formed by the $1B_u$ oscillator and some A_g oscillators, and given by

$$\rho^{(0|2)}(t)=e^{-2i\omega_2 t}\left(\frac{1}{2}([[\xi_1,\overline{\rho}],\xi_1]+[[\xi_1,\overline{\rho}],\xi_1])(z_1^{(0|1)}(t))^2 + \sum_\beta \xi_\beta z_\beta^{(0|2)}(t)\right). \tag{30}$$

The density matrix consists of small contribution from the $1B_u$ and about mainly two A_g oscillators, namely $3A_g$ and $5A_g$. Its shape is essentially a superposition of the density matrices representing the $3A_g$ and the $5A_g$ oscillators, shown in Fig. 2.

Having analyzed the different contributions to the nonlinear optical response within the PPP model, we propose a simplified two-oscillator model,[16] which to a good accuracy reproduces the signal. Compared to the model resulting from the elimination of off-resonant contributions, we further neglect small contributions like X_1, $X_{-1,}$ and Y_1, and also s_2 and its renormalization X_3 and Y_3. We further neglect the anharmonic constants A_1, A_2, A_3, B_1, and B_2 that appear in the definition of the polarization. So now the off-resonant oscillators only enter in renormalizations of s_1 and V_1. The equations considered within this reduced model are[16]

$$i\frac{\partial}{\partial t}z_1=\left(\Omega_1-\omega_L-i\frac{1}{T_2}\right)z_1-\mu_1 E-E\mu_{12}z_2-E(s_1+Y_2+X_2)z_1z_{-1}+2V_{12}z_2z_{-1}+(V_1+Y_4+X_4)z_{-1}z_1z_1, \tag{31}$$

$$z_{-1}=z_1^*,$$

$$i\frac{\partial}{\partial t}z_2=\left(\Omega_2-2\omega_L-i\frac{1}{T_2'}\right)z_2-E\mu_{12}z_1+V_{12}z_1z_1. \tag{32}$$

The induced polarization is given by

$$P_S(t)=e^{-i\omega_L t}(\mu_1 z_1+\mu_{12}z_2z_{-1}). \tag{33}$$

We compare the results obtained for this model (IVP) with results obtained by a full calculation (VP), where we have kept all oscillators explicitly (in practice these results were obtained by a real-space calculation), see Appendix B. The good agreement between the two calculations shown in Fig. 11, confirms the validity of this simplified description. There are only slight differences in the amplitude and the phase of the FWM signal mainly during the initial excitation process.

Another important effect is the existence of strong FWM signals for negative delays, which may be induced by either two-photon A_g oscillator variables, or by many-body anharmonicities of the B_u oscillators. Our calculations show that, as for positive delay, the many-body anharmonicities contribute most strongly to the signal for negative delays. The time-integrated signals in Fig. 12 decay for positive delays

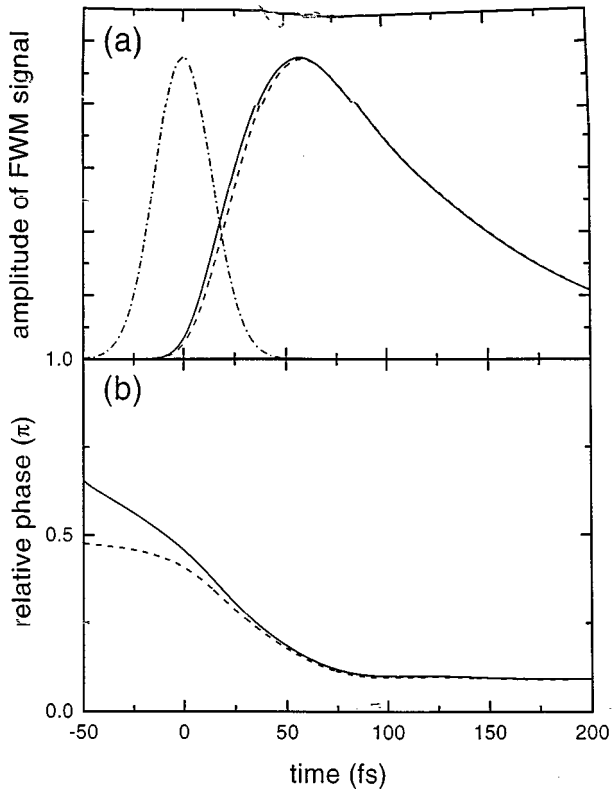

FIG. 11. (a) Time-resolved amplitude and (b) phase of the FWM signal for time-delay $\tau=0$ fs for the PPP model. Solid line: model VP, dashed: model IVP, and dashed-dotted: laser pulse envelope.

with $T_2/2$, and for negative delays with about $T_2/4$.[18,19] The very weak modulations, which can be seen for negative delays, are due to quantum beats with a frequency determined by $2\Omega(1B_u)-\Omega(5A_g)$. The results for the full model VP (solid line) and the reduced model IVP (dashed line) are again in very good agreement.

IV. SUMMARY

In summary, we have modeled resonant two-pulse four-wave mixing experiments in conjugated polyenes using the electronic-oscillator representation. We found that it is only required to consider two electronic oscillators explicitly. The role of electronic correlations has been clarified by comparing calculations done in the absence of electronic correlations (Hückel model) and with strong electronic correlations (PPP model). While both models have similar linear optical properties, i.e., a strong lowest transition at the same spectral position, their nonlinear optical properties are very different. For the PPP model we predict signatures of electronic correlations, which should be observable in ultrafast optical spectroscopy, in both the phase and the amplitude of the signal. We expect analogous effects to be observable using frequency-domain resonant four-wave mixing techniques.[39] The coupling coefficients leading to the nonlinear optical response as well as the calculated signals have been compared to theoretical and experimental treatments for inorganic semiconductors. The present approach provides a unified theoretical analysis of resonant nonlinear experiments in organic and inorganic materials.

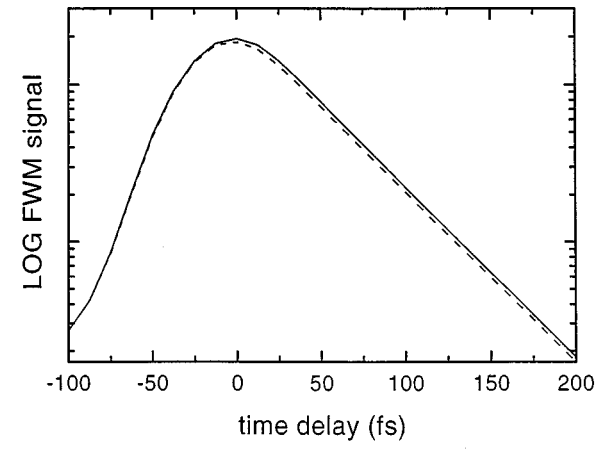

FIG. 12. Time-integrated FWM for the PPP model. Solid line: model VP, dashed: model IVP.

ACKNOWLEDGMENTS

The support of the Air Force Office of Scientific Research, and the National Science Foundation through Grants Nos. CHE-9526125 and PHY94-15583 is gratefully acknowledged. T.M. acknowledges financial support from NATO through the Deutscher Akademischer Austauschdienst (DAAD).

APPENDIX A: EQUATIONS OF MOTION FOR TWO-PULSE NONLINEAR OPTICAL RESPONSE

In this appendix, we show how the oscillator equations of motion can be used to describe multiple-pulse optical experiments. We consider a two-pulse nonlinear optical experiment, where the exciting field is given by

$$\begin{aligned} E(t) &= E_1(t)(e^{i\mathbf{k}_1\cdot\mathbf{r}-i\omega_1 t}+e^{-i\mathbf{k}_1\cdot\mathbf{r}+i\omega_1 t}) \\ &\quad + E_2(t)(e^{i\mathbf{k}_2\cdot\mathbf{r}-i\omega_2 t}+e^{-i\mathbf{k}_2\cdot\mathbf{r}+i\omega_2 t}) \\ &= E_1^+(t)e^{-i\omega_1 t}+E_1^-(t)e^{i\omega_1 t} \\ &\quad + E_2^+(t)e^{-i\omega_2 t}+E_2^-(t)e^{i\omega_2 t}. \end{aligned} \tag{A1}$$

$E_{1,2}(t)$ are the pulse envelopes. The term E_i^+ (E_i^-) refer to the components of E with direction $+\mathbf{k}_i$ ($-\mathbf{k}_i$). Such an exciting field will create excitations associated with different directions $e^{i\mathbf{K}\cdot\mathbf{r}}$, $\mathbf{K}=n\mathbf{k}_1+m\mathbf{k}_2$, where n,m can be any integers.[20,40] We label these different directional components by $^{(n|m)}$, which refers to the excitation associated with the direction $n\mathbf{k}_1+m\mathbf{k}_2$. Inserting this decomposition into the equations of motion, Eq. (15), and transforming to the rotating frame leads to

$$
\begin{aligned}
i\frac{\partial}{\partial t}z_{\alpha}^{(n|m)} &= (\Omega_{\alpha}-n\omega_1-m\omega_2)z_{\alpha}^{(n|m)}-\mu_{\alpha}(\delta_{n=1}\delta_{m=0}E_1^{+}+\delta_{n=-1}\delta_{m=0}E_1^{-}+\delta_{n=0}\delta_{m=1}E_2^{+}+\delta_{n=0}\delta_{m=-1}E_2^{-})\\
&-E_1^{+}\sum_{\beta}\mu_{\alpha,\beta}z_{\beta}^{(n-1|m)}-E_1^{-}\sum_{\beta}\mu_{\alpha,\beta}z_{\beta}^{(n+1|m)}-E_2^{+}\sum_{\beta}\mu_{\alpha,\beta}z_{\beta}^{(n|m-1)}-E_2^{-}\sum_{\beta}\mu_{\alpha,\beta}z_{\beta}^{(n|m+1)}\\
&-E_1^{+}\sum_{n'm'\beta\gamma}\mu_{\alpha,\beta\gamma}z_{\beta}^{(n-n'-1|m-m')}z_{\gamma}^{(n'|m')}-E_1^{-}\sum_{n'm'\beta\gamma}\mu_{\alpha,\beta\gamma}z_{\beta}^{(n-n'+1|m-m')}z_{\gamma}^{(n'|m')}\\
&-E_2^{+}\sum_{n'm'\beta\gamma}\mu_{\alpha,\beta\gamma}z_{\beta}^{(n-n'|m-m'-1)}z_{\gamma}^{(n'|m')}-E_2^{-}\sum_{n'm'\beta\gamma}\mu_{\alpha,\beta\gamma}z_{\beta}^{(n-n'|m-m'+1)}z_{\gamma}^{(n'|m')}\\
&+\sum_{n'm'\beta\gamma}V_{\alpha,\beta\gamma}z_{\beta}^{(n-n'|m-m')}z_{\gamma}^{(n'|m')}+\sum_{n'm'n''m''\beta\gamma\delta}V_{\alpha,\beta\gamma\delta}z_{\beta}^{(n-n'-n''|m-m'-m'')}z_{\gamma}^{(n'|m')}z_{\delta}^{(n''|m'')}. \qquad \text{(A2)}
\end{aligned}
$$

The polarization is given by

$$
P^{(n|m)}(t)=e^{i(n\mathbf{k}_1+m\mathbf{k}_2)\cdot\mathbf{r}-i(n\omega_1+m\omega_2)t}\Bigg(\sum_{\beta}\tilde{\mu}_{\beta}z_{\beta}^{(n|m)}+\sum_{n',m',\beta\gamma}\tilde{\mu}_{\beta\gamma}z_{\beta}^{(n-n'|m-m')}z_{\gamma}^{(n'|m')}\Bigg). \qquad \text{(A3)}
$$

These equations can be used to describe two pulse experiments; the generalization to experiments with more than two exciting pulses is straightforward. In Eq. (A2) we have only to solve explicitly for the complex amplitudes of the oscillator variables associated with positive frequency ($\alpha>0$). The amplitudes for the corresponding modes with negative frequencies are determined by $z_{-\alpha}^{(n|m)}=(z_{\alpha}^{(-n|-m)})^{*}$. Here, $-\alpha$ refers to the adjoint mode of α. All oscillator variables and amplitudes have to be included in the summations appearing on right-hand sides of Eqs. (A2) and (A3).

APPENDIX B: ITERATIVE CALCULATION OF THE FOUR-WAVE MIXING SIGNAL

In the following we perform a detailed analysis of FWM in self-diffraction geometry, where the third-order signal is monitored in the direction $2\mathbf{k}_2-\mathbf{k}_1$. Only B_u oscillators can be excited in the linear response,

$$
\begin{aligned}
i\frac{\partial}{\partial t}z_{\alpha}^{(1|0)} &= (\Omega_{\alpha}-\omega_1)z_{\alpha}^{(1|0)}-\mu_{\alpha}E_1^{+},\\
i\frac{\partial}{\partial t}z_{\alpha}^{(-1|0)} &= (\Omega_{\alpha}+\omega_1)z_{\alpha}^{(-1|0)}-\mu_{\alpha}E_1^{-},\\
i\frac{\partial}{\partial t}z_{\alpha}^{(0|1)} &= (\Omega_{\alpha}-\omega_2)z_{\alpha}^{(0|1)}-\mu_{\alpha}E_2^{+},\\
i\frac{\partial}{\partial t}z_{\alpha}^{(0|-1)} &= (\Omega_{\alpha}+\omega_2)z_{\alpha}^{(0|-1)}-\mu_{\alpha}E_2^{-},\\
z_{-\alpha}^{(1|0)} &= (z_{\alpha}^{(-1|0)})^{*},\\
z_{-\alpha}^{(-1|0)} &= (z_{\alpha}^{(1|0)})^{*},\\
z_{-\alpha}^{(0|1)} &= (z_{\alpha}^{(0|-1)})^{*},\\
z_{-\alpha}^{(0|-1)} &= (z_{\alpha}^{(0|1)})^{*}. \qquad \text{(B1)}
\end{aligned}
$$

The second order response consists of different contributions. The particle-particle part is given by $T(\xi)$ and has not to be calculated separately, but is completely determined by the linear response.[12] Additionally A_g oscillators can be excited in second order, representing the particle-hole part of the response. To calculate the FWM signal in the direction $2\mathbf{k}_2-\mathbf{k}_1$ in third order, we have to consider a transient-grating ($\mathbf{k}_2-\mathbf{k}_1$; $\omega_1-\omega_2$) and a two-photon ($2\mathbf{k}_2$; $-2\omega_2$) response.

$$
\begin{aligned}
i\frac{\partial}{\partial t}z_{\alpha}^{(-1|1)} &= (\Omega_{\alpha}+\omega_1-\omega_2)z_{\alpha}^{(-1|1)}-E_1^{-}\sum_{\beta}\mu_{\alpha,\beta}z_{\beta}^{(0|1)}\\
&-E_2^{+}\sum_{\beta}\mu_{\alpha,\beta}z_{\beta}^{(-1|0)}\\
&+\sum_{\beta\gamma}(V_{\alpha,\beta\gamma}+V_{\alpha,\gamma\beta})z_{\beta}^{(-1|0)}z_{\gamma}^{(0|1)},\\
i\frac{\partial}{\partial t}z_{\alpha}^{(1|-1)} &= (\Omega_{\alpha}-\omega_1+\omega_2)z_{\alpha}^{(1|-1)}-E_1^{+}\sum_{\beta}\mu_{\alpha,\beta}z_{\beta}^{(0|-1)}\\
&-E_2^{-}\sum_{\beta}\mu_{\alpha,\beta}z_{\beta}^{(1|0)}+\sum_{\beta\gamma}(V_{\alpha,\beta\gamma}\\
&+V_{\alpha,\gamma\beta})z_{\beta}^{(1|0)}z_{\gamma}^{(0|-1)},\\
i\frac{\partial}{\partial t}z_{\alpha}^{(0|2)} &= (\Omega_{\alpha}-2\omega_2)z_{\alpha}^{(0|2)}-E_2^{+}\sum_{\beta}\mu_{\alpha,\beta}z_{\beta}^{(0|1)}\\
&+\sum_{\beta\gamma}V_{\alpha,\beta\gamma}z_{\beta}^{(0|1)}z_{\gamma}^{(0|1)},\\
i\frac{\partial}{\partial t}z_{\alpha}^{(0|-2)} &= (\Omega_{\alpha}+2\omega_2)z_{\alpha}^{(0|-2)}-E_2^{-}\sum_{\beta}\mu_{\alpha,\beta}z_{\beta}^{(0|-1)}\\
&+\sum_{\beta\gamma}V_{\alpha,\beta\gamma}z_{\beta}^{(0|-1)}z_{\gamma}^{(0|-1)},\\
z_{-\alpha}^{(-1|1)} &= (z_{\alpha}^{(1|-1)})^{*},\\
z_{-\alpha}^{(1|-1)} &= (z_{\alpha}^{(-1|1)})^{*},\\
z_{-\alpha}^{(0|2)} &= (z_{\alpha}^{(0|-2)})^{*},\\
z_{-\alpha}^{(0|-2)} &= (z_{\alpha}^{(0|2)})^{*}. \qquad \text{(B2)}
\end{aligned}
$$

In third order again, only B_u oscillators can be excited,

$$i\frac{\partial}{\partial t}z_\alpha^{(-1|2)}=(\Omega_\alpha+\omega_1-2\omega_2)z_\alpha^{(-1|2)}-E_1^-\sum_\beta \mu_{\alpha,\beta}z_\beta^{(0|2)}-E_2^+\sum_\beta \mu_{\alpha,\beta}z_\beta^{(-1|1)}-E_1^-\sum_{\beta\gamma} \mu_{\alpha,\beta\gamma}z_\beta^{(0|1)}z_\gamma^{(0|1)}$$

$$-E_2^+\sum_{\beta\gamma}(\mu_{\alpha,\beta\gamma}+\mu_{\alpha,\gamma\beta})z_\beta^{(-1|0)}z_\gamma^{(0|1)}+\sum_{\beta\gamma}(V_{\alpha,\beta\gamma}+V_{\alpha,\gamma\beta})z_\beta^{(0|2)}z_\gamma^{(-1|0)}+\sum_{\beta\gamma}(V_{\alpha,\beta\gamma}+V_{\alpha,\gamma\beta})z_\beta^{(-1|1)}z_\gamma^{(0|1)}$$

$$+\sum_{\beta\gamma\delta}(V_{\alpha,\beta\gamma\delta}+V_{\alpha,\gamma\beta\delta}+V_{\alpha,\gamma\delta\beta})z_\beta^{(-1|0)}z_\gamma^{(0|1)}z_\delta^{(0|1)},$$

$$i\frac{\partial}{\partial t}z_\alpha^{(1|-2)}=(\Omega_\alpha-\omega_1+2\omega_2)z_\alpha^{(1|-2)}-E_1^+\sum_\beta \mu_{\alpha,\beta}z_\beta^{(0|-2)}-E_2^-\sum_\beta \mu_{\alpha,\beta}z_\beta^{(1|-1)}-E_1^+\sum_{\beta\gamma} \mu_{\alpha,\beta\gamma}z_\beta^{(0|-1)}z_\gamma^{(0|-1)}$$

$$-E_2^-\sum_{\beta\gamma}(\mu_{\alpha,\beta\gamma}+\mu_{\alpha,\gamma\beta})z_\beta^{(1|0)}z_\gamma^{(0|-1)}+\sum_{\beta\gamma}(V_{\alpha,\beta\gamma}+V_{\alpha,\gamma\beta})z_\beta^{(0|-2)}z_\gamma^{(1|0)}+\sum_{\beta\gamma}(V_{\alpha,\beta\gamma}+V_{\alpha,\gamma\beta})z_\beta^{(1|-1)}z_\gamma^{(0|-1)}$$

$$+\sum_{\beta\gamma\delta}(V_{\alpha,\beta\gamma\delta}+V_{\alpha,\gamma\beta\delta}+V_{\alpha,\gamma\delta\beta})z_\beta^{(1|0)}z_\gamma^{(0|-1)}z_\delta^{(0|-1)},$$

$$z_{-\alpha}^{(-1|2)}=(z_\alpha^{(1|-2)})^*,$$

$$z_{-\alpha}^{(1|-2)}=(z_\alpha^{(-1|2)})^*. \tag{B3}$$

The polarization in the $2\mathbf{k}_2-\mathbf{k}_1$ direction is finally given by

$$P^{(-1|2)}(t)=e^{i(-\mathbf{k}_1+2\mathbf{k}_2)\cdot\mathbf{r}-i(-\omega_1+2\omega_2)t}\left(\sum_\beta \tilde{\mu}_\beta z_\beta^{(-1|2)}+\sum_{\beta\gamma}(\tilde{\mu}_{\beta\gamma}+\tilde{\mu}_{\gamma\beta})(z_\beta^{(-1|0)}z_\gamma^{(0|2)}+z_\beta^{(0|1)}z_\gamma^{(-1|1)})\right). \tag{B4}$$

Equations (B3) and (B4) include all resonant and nonresonant pathways that can contribute to the two-pulse FWM experiment considered here.

APPENDIX C: ELIMINATION OF OFF-RESONANT OSCILLATORS

Below we describe how the general equations of motion of Appendix B can be reduced to include only the relevant oscillators, which are needed for the description of resonant FWM. In our numerical calculations we have assumed that the central frequency of both exciting pulses is in resonance with the transition to the $1B_u$ oscillator, i.e., $\omega_L=\omega_1=\omega_2=\Omega(1B_u)$. The pulse envelopes are assumed to be Gaussian, $E(t)\propto e^{-[(t-\hat{t})/\bar{t}]^2}$, with a width of $\bar{t}=20$ fs. Since the spectral width of even these very short laser pulses (about 0.1 eV) is small compared to the frequency spacing between the dominant oscillators, only a few oscillators will be excited resonantly. Our calculations show that the first and third order response is to very good accuracy dominated by only the $1B_u$ oscillator. In second order there may be one A_g oscillator which appears as resonantly excited two-photon transition. We now develop equations which only retain two primary oscillators, the $1B_u$ and one A_g oscillator explicitly. The off-resonant contributions from all other A_g oscillators in second order, can be eliminated from the equations of motion and will result in renormalization of anharmonicities and scattering constants.

The elimination of the off-resonant oscillators goes as follows: In the equation of motion for the two-photon resonances $z_\alpha^{(0|2)}$ we assume that the amplitude adiabatically follows its inhomogeneity on the right hand side of the equation. So we can set $(\partial/\partial t)z_\alpha^{(0|2)}=0$ and then solve the equation, which gives

$$z_\alpha^{(0|2)}=\frac{1}{\Omega_\alpha-2\omega_L}(E_2^+\mu_{\alpha,1}z_1^{(0|1)}-V_{\alpha,11}z_1^{(0|1)}z_1^{(0|1)}) \tag{C1}$$

The contributions of A_g oscillator variables associated with negative frequency are given by

$$z_{-\alpha}^{(0|2)}=\frac{1}{\Omega_\alpha+2\omega_L}(E_2^+\mu_{\alpha,-1}z_1^{(0|1)}-V_{\alpha,-1-1}z_1^{(0|1)}z_1^{(0|1)}). \tag{C2}$$

Here the index 1 refers to the positive frequency oscillator variable of $1B_u$ oscillator and -1 to its adjoint, i.e. the negative frequency variable.

The similar elimination can be done for the transient-grating like terms. Here all oscillators can be assumed to be off resonant, since there is no particle-hole oscillator with zero frequency,

$$z_\alpha^{(-1|1)}=\frac{1}{\Omega_\alpha}(E_1^-\mu_{\alpha,1}z_1^{(0|1)}+E_2^+\mu_{\alpha,-1}z_{-1}^{(-1|0)}$$

$$-(V_{\alpha,1-1}+V_{\alpha,-11})z_{-1}^{(-1|0)}z_1^{(0|1)}) \tag{C3}$$

and

$$z_{-\alpha}^{(-1|1)}=\frac{1}{\Omega_\alpha}[E_1^-\mu_{\alpha,-1}z_1^{(0|1)}+E_2^+\mu_{\alpha,1}z_{-1}^{(-1|0)} -(V_{\alpha,-11}+V_{\alpha,1-1})z_{-1}^{(-1|0)}z_1^{(0|1)}]. \quad \text{(C4)}$$

These expressions for the off-resonant second order quantities can be inserted into the equation for the third order amplitude, which leads to the renormalization of some nonlinear coupling constants and a few additional terms. After this elimination, keeping just two oscillators explicitly (1 refers to the $1B_u$ oscillator and 2 the A_g considered as a two-photon resonance), the FWM signal is determined by the following set of equations. In first order,

$$i\frac{\partial}{\partial t}z_1^{(1|0)}=(\Omega_1-\omega_L)z_1^{(1|0)}-\mu_1E_1^+,$$

$$z_{-1}^{(-1|0)}=(z_1^{(1|0)})^*,$$

$$i\frac{\partial}{\partial t}z_1^{(0|1)}=(\Omega_1-\omega_L)z_1^{(0|1)}-\mu_1E_2^+,$$

$$z_{-1}^{(0|-1)}=(z_1^{(0|1)})^*. \quad \text{(C5)}$$

In second order,

$$i\frac{\partial}{\partial t}z_2^{(0|2)}=(\Omega_2-2\omega_L)z_2^{(0|2)}-E_2^+\mu_{12}z_1^{(0|1)}+V_{12}z_1^{(0|1)}z_1^{(0|1)}. \quad \text{(C6)}$$

And in third order,

$$i\frac{\partial}{\partial t}z_1^{(-1|2)}=(\Omega_1-\omega_L)z_1^{(-1|2)}-E_1^-E_2^+(Y_1+X_1)z_1^{(0|1)}-(E_2^+)^2(X_{-1})z_{-1}^{(-1|0)}-E_1^-\mu_{12}z_2^{(0|2)}-E_1^-(s_2+Y_3+X_3)z_1^{(0|1)}z_1^{(0|1)}$$
$$-E_2^+(s_1+Y_2+X_2)z_{-1}^{(-1|0)}z_1^{(0|1)}+2V_{12}z_2^{(0|2)}z_{-1}^{(-1|0)}+(V_1+Y_4+X_4)z_{-1}^{(-1|0)}z_1^{(0|1)}z_1^{(0|1)}. \quad \text{(C7)}$$

The polarization in the direction is given by

$$P^{(-1|2)}(t)=e^{i(-\mathbf{k}_1+2\mathbf{k}_2)\cdot\mathbf{r}-i(-\omega_1+2\omega_2)t}\left(\mu_1z_1^{(-1|2)}+\sum_\beta\mu_{1\beta}z_{-1}^{(-1|0)}z_\beta^{(0|2)}+\sum_\beta\mu_{-1\beta}z_1^{(0|1)}z_\beta^{(-1|1)}\right). \quad \text{(C8)}$$

In these equations we have used some abreviations:

$$\mu_1=\tilde{\mu}_1,$$

$$\mu_{1n}=\mu_{1,n}=\mu_{n,1}=(\tilde{\mu}_{-1n}+\tilde{\mu}_{n-1}),$$

$$s_1=(\mu_{1,-11}+\mu_{1,1-1}),$$

$$s_2=\mu_{1,11},$$

$$V_1=(V_{1,11-1}+V_{1,1-11}+V_{1,-111}),$$

$$V_{12}=V_{2,11}=\frac{1}{2}(V_{1,-12}+V_{1,2-1}). \quad \text{(C9)}$$

The quantities X_i and Y_i result from the elimination of the transient grating and two-photon resonances, respectively. They are given by the following summations over the A_g oscillator variables β:

$$X_1=\sum_\beta\frac{\mu_{1,\beta}\mu_{\beta,1}+\mu_{1,-\beta}\mu_{\beta,-1}}{\Omega_\beta},$$

$$X_{-1}=\sum_\beta\frac{\mu_{1,\beta}\mu_{\beta,-1}+\mu_{1,-\beta}\mu_{\beta,1}}{\Omega_\beta},$$

$$X_2=\sum_\beta \frac{-1}{\Omega_\beta}[\mu_{1,\beta}(V_{\beta,-11}+V_{\beta,1-1})+\mu_{\beta,-1}(V_{1,\beta1}+V_{1,1\beta})+\mu_{1,-\beta}(V_{\beta,1-1}+V_{\beta,-11})+\mu_{\beta,1}(V_{1,-\beta1}+V_{1,1-\beta})],$$

$$X_3=\sum_\beta \frac{-1}{\Omega_\beta}[\mu_{\beta,1}(V_{1,\beta1}+V_{1,1\beta})+\mu_{\beta,-1}(V_{1,-\beta1}+V_{1,1-\beta})],$$

$$X_4=\sum_\beta \frac{-1}{\Omega_\beta}[(V_{\beta,-11}+V_{\beta,1-1})(V_{1,\beta1}+V_{1,1\beta})+(V_{\beta,1-1}+V_{\beta,-11})(V_{1,-\beta1}+V_{1,1-\beta})],$$

$$Y_1=\sum_\beta{}' \frac{1}{\Omega_\beta-2\omega_L}\mu_{1,\beta}\mu_{\beta,1}+\sum_\beta \frac{1}{\Omega_\beta+2\omega_L}\mu_{1,-\beta}\mu_{\beta,-1},$$

$$Y_2=\sum_\beta{}' \frac{-1}{\Omega_\beta-2\omega_L}\mu_{\beta,1}(V_{1,\beta-1}+V_{1,-1\beta})+\sum_\beta \frac{-1}{\Omega_\beta+2\omega_L}\mu_{\beta,-1}(V_{1,-\beta-1}+V_{1,-1-\beta}),$$

$$Y_3=\sum_\beta{}' \frac{-1}{\Omega_\beta-2\omega_L}\mu_{1,\beta}V_{\beta,11}+\sum_\beta \frac{-1}{\Omega_\beta+2\omega_L}\mu_{1,-\beta}V_{\beta,-1-1},$$

$$Y_4=\sum_\beta{}' \frac{-1}{\Omega_\beta-2\omega_L}(V_{1,\beta-1}+V_{1,-1\beta})V_{\beta,11}+\sum_\beta \frac{-1}{\Omega_\beta+2\omega_L}(V_{1,-\beta-1}+V_{1,-1-\beta})V_{\beta,-1-1}. \quad \text{(C10)}$$

The primes over the sum symbols for Y_i indicate, that the summations exclude the positive frequency variable of the one A_g oscillator, which is explicitly considered as a two-photon resonance. In Sec. III we show, that to a very good accuracy the approximate equations derived in this Appendix reproduce the full results calculated using Eqs. (B1)–(B4).

Inserting the expressions for the amplitudes of the virtual oscillators Eqs. (C1)–(C4) into Eq. (C9) allows to perform the summations over β and simplifies the expression for the polarization. As in the equations of motion, this procedure results in some alternative anharmonic couplings:

$$P^{(-1|2)}(t)=e^{i(-\mathbf{k}_1+2\mathbf{k}_2)\cdot\mathbf{r}-i(-\omega_1+2\omega_2)t}[\mu_1 z_1^{(-1|2)}+\mu_{12}z_{-1}^{(-1|0)}z_2^{(0|2)}+(A_1+B_1)z_{-1}^{(-1|0)}(z_1^{(0|1)})^2+(A_2+B_2)E_2^+ z_{-1}^{(-1|0)}z_1^{(0|1)}+A_3E_1^-(z_1^{(0|1)})^2]. \quad \text{(C11)}$$

Here A_1, A_2, and A_3 are obtained via elimination of the transient-grating terms involving virtual oscillators, and B_1, as well as B_2 from the corresponding two-photon terms.

[1] *Proceedings of the NATO Advanced Research Workshop Conjugated Polymeric Materials: Opportunities in Electronics, Optoelectronics, and Molecular Electronics*, Vol. 182 of *NATO Advanced Study Institute, Series E: Applied Sciences*, edited by J.L. Bredás and R.R. Chance, (Kluwer, Dordrecht, 1990).

[2] Chem. Phys. **210** (No. 1, 2), special issue on Confined Excitations in Molecular and Semiconductor Nanostructures, edited by S. Mukamel and D.S. Chemla.

[3] G.M. Carter, J.V. Hryniewicz, M.K. Thakur, Y.J. Chen, and S.E. Meyler, Appl. Phys. Lett. **49**, 998 (1986); J.M. Huxley, P. Mataloni, R.W. Schoenlein, J.G. Fujimoto, E.P. Ippen, and G.M. Carter, *ibid.* **56**, 1600 (1990).

[4] M. Yan, L.J. Rothberg, F. Papadimitrakopoulos, M.E. Galvin, and T.M. Miller, Phys. Rev. Lett. **72**, 1104 (1994); **73**, 744 (1994); M. Yan, L.J. Rothberg, E.W. Kwock, and T.M. Miller, *ibid.* **75**, 1992 (1995).

[5] R. Kersting, U. Lemmer, R.F. Mahrt, K. Leo, H. Kurz, H. Bässler, and E.O. Göbel, Phys. Rev. Lett. **70**, 3820 (1993); U. Lemmer, R.F. Mahrt, Y. Wada, A. Greiner, H. Bässler, and E.O. Göbel, Chem. Phys. Lett. **209**, 243 (1993); R. Kersting, U. Lemmer, M. Deussen, H.J. Bakker, R.F. Mahrt, H. Kurz, V.I. Arkhipov, H. Bässler, and E.O. Göbel, Phys. Rev. Lett. **73**, 1440 (1994).

[6] (a) S.K. Ghoshal, P. Chopra, B.P. Singh, J. Swiatkiewicz, and P.N. Prasad, J. Chem. Phys. **90**, 5078 (1989); (b) M. Samoc and P.N. Prasad, *ibid.* **91**, 6643 (1989).

[7] T.A. Pham, A. Daunois, J.-C. Merle, J. Le Moigne, and Y.-V. Bigot, Phys. Rev. Lett. **74**, 904 (1995).

[8] Z.G. Soos, S. Ramesesha, D.S. Galvao, and S. Etemad, Phys. Rev. B **47**, 1742 (1993).

[9] J.F. Heflin, K.Y. Wong, Q. Zamani-Khamiri, and A.F. Garito, Phys. Rev. B **38**, 1573 (1988); D.C. Rodenberger and A.F. Garito, Nature **359**, 309 (1992).

[10] J.L. Bredás, C. Adant, P. Tackx, A. Persoons, and B.M. Pierce, Chem. Rev. **94**, 243 (1994).

[11] P. Ring and P. Schuck, *The Nuclear Many-Body Problem* (Springer, New York, 1980).

[12] V. Chernyak and S. Mukamel, J. Chem. Phys **104**, 444 (1996).

[13] A. Takahashi and S. Mukamel, J. Chem. Phys. **100**, 2366 (1994).

[14] S. Mukamel, A. Takahashi, H.X. Wang, and G. Chen, Science **166**, 251 (1994).
[15] S. Tretiak, V. Chernyak, and S. Mukamel, Chem. Phys. Lett. **259**, 55 (1996); J. Chem. Phys. **105**, 8914 (1996).
[16] T. Meier and S. Mukamel, Phys. Rev. Lett. **77**, 3471 (1996).
[17] A.J. Heeger, S. Kivelson, J.R. Schrieffer, and W.-P. Su, Rev. Mod. Phys. **60**, 781 (1988).
[18] M. Wegener, D.S. Chemla, S. Schmitt-Rink, and W. Schäfer, Phys. Rev. A **42**, 5675 (1990).
[19] S. Schmitt-Rink, S. Mukamel, K. Leo, J. Shah, and D.S. Chemla, Phys. Rev. A **44**, 2124 (1991).
[20] M. Lindberg, R. Binder, and S.W. Koch, Phys. Rev. A **45**, 1865 (1992).
[21] S. Weiss, M.-A. Mycek, J.-Y. Bigot, S. Schmitt-Rink, and D.S. Chemla, Phys. Rev. Lett. **69**, 2685 (1992).
[22] D.-S. Kim, J. Shah, T.C. Damen, W. Schäfer, F. Jahnke, S. Schmitt-Rink, and K. Köhler, Phys. Rev. Lett. **69**, 2725 (1992).
[23] K. Bott, O. Heller, D. Bennhardt, S.T. Cundiff, P. Thomas, E.J. Mayer, G.O. Smith, R. Eccleston, J. Kuhl, and K. Ploog, Phys. Rev. B **49**, 7817 (1993); E.J. Mayer, G.O. Smith, V. Heuckeroth, J. Kuhl, K. Bott, A. Schulze, T. Meier, D. Bennhardt, S.W. Koch, P. Thomas, R. Hey, and K. Ploog, *ibid.* **50**, 14 730 (1994).
[24] J.A. Leegwater and S. Mukamel, J. Chem. Phys. **101**, 7388 (1994).
[25] O. Kühn, V. Chernyak, and S. Mukamel, J. Chem. Phys. **105**, 8586 (1996).
[26] H. Fukutome, J. Mol. Struct. (Theochem.) **188**, 377 (1989), and references therein.
[27] The geometry optimization enters into the Hamiltonian by a term $\frac{1}{2}\Sigma_n K(x_n-\overline{x})^2$, where x_n is the nth bond length, we have used a force constant of $K=21$ eV Å($K=38$ eV Å) for the Hückel (PPP) model and an equilibrium bond length of $\overline{x}=1.41$ Å for both models, see Ref. 13.
[28] G. Chen and S. Mukamel, Chem. Phys. Lett. **240**, 296 (1995).
[29] S. Mukamel, *Principles of Nonlinear Optical Spectroscopy* (Oxford, New York, 1995).
[30] D.S. Chemla, J.-Y. Bigot, M.-A. Mycek, S. Weiss, and W. Schäfer, Phys. Rev. B **50**, 8439 (1994).
[31] L. Allen and J.H. Eberly, *Optical Resonances and Two-Level Atoms* (Wiley, New York, 1975).
[32] T. Yajima and Y. Taira, J. Phys. Soc. Jpn. **47**, 1620 (1979).
[33] W. Huhn and A. Stahl, Phys. Status Solidi B **124**, 167 (1984); S. Schmitt-Rink, D.S. Chemla, and H. Haug, Phys. Rev. B **37**, 941 (1988); M. Lindberg and S.W. Koch, *ibid.* **38**, 3342 (1988).
[34] For a textbook discussion of the semiconductor Bloch equations, see H. Haug and S.W. Koch, *Quantum Theory of the Optical and Electronic Properties of Semiconductors* (World Scientific, Singapore, 1994), 3rd ed.
[35] F. Jahnke, M. Koch, T. Meier, J. Feldmann, W. Schäfer, P. Thomas, S.W. Koch, E.O. Göbel, and H. Nickel, Phys. Rev. B **50**, 8114 (1994).
[36] J.-Y. Bigot M.-A. Mycek, S. Weiss, R.G. Ulbrich, and D.S. Chemla, Phys. Rev. Lett. **70**, 3307 (1993).
[37] *Selected Papers on Coherence and Fluctuations of Light, with Bibliography*, edited by L. Mandel and E. Wolf (Dover Publications, 1970).
[38] L. Cohen, Proc. IEEE **77**, 941 (1989).
[39] W.E. Torruelas, D. Neher, R. Zanoni, G.I. Stegeman, and F. Kajzar, Chem. Phys. Lett. **175**, 11 (1990); M. Cha, W.E. Torruelas, G.I. Stegeman, H.X. Wang, A. Takahashi, and S. Mukamel, *ibid.* **228**, 73 (1994); M.A. Díaz-García, I. Ledoux, F. Fernández-Lázaro, A. Sastre, T. Torres, F. Agulló-López, and J. Zyss, J. Phys. Chem. **98**, 4495 (1994); M.A. Díaz-García, I. Ledoux, J.A. Duro, T. Torres, F. Agulló-López, and J. Zyss, *ibid.* **98**, 8761 (1994); M.A. Díaz-García, F. Agulló-López, W.E. Torruellas, and G.I. Stegeman, Chem. Phys. Lett. (to be published).
[40] S. Mukamel and R.F. Loring, J. Opt. Soc. B **3**, 595 (1986).